

# Competing $p$ -wave orders

Aristomenis Donos<sup>1</sup>, Jerome P. Gauntlett<sup>2</sup> and Christiana Pantelidou<sup>2</sup>

<sup>1</sup>*DAMTP, University of Cambridge  
Cambridge, CB3 0WA, U.K.*

<sup>2</sup>*Blackett Laboratory, Imperial College  
London, SW7 2AZ, U.K.*

## Abstract

We construct electrically charged, asymptotically  $AdS_5$  black hole solutions that are dual to  $d = 4$  CFTs in a superfluid phase with either  $p$ -wave or  $(p + ip)$ -wave order. The two types of black holes have non-vanishing charged two-form in the bulk and appear at the same critical temperature in the unbroken phase. Both the  $p$ -wave and the  $(p + ip)$ -wave phase can be thermodynamically preferred, depending on the mass and charge of the two-form, and there can also be first order transitions between them. The  $p$ -wave black holes have a helical structure and some of them exhibit the phenomenon of pitch inversion as the temperature is decreased. Both the  $p$ -wave and the  $(p + ip)$ -wave black holes have zero entropy density ground states at zero temperature and we identify some new ground states which exhibit scaling symmetry, including a novel scenario for the emergence of conformal symmetry in the IR.

# 1 Introduction

Investigating the thermal properties of strongly coupled matter using holographic techniques has revealed an extraordinarily rich landscape of novel black hole solutions and it seems likely that we have still only seen the tip of the iceberg.

An interesting class of examples involve strongly coupled conformal field theories (CFTs) in flat spacetime when held at finite chemical potential with respect to a global  $U(1)$  symmetry. These are described by electrically charged, asymptotically AdS black holes with event horizons that are topologically planar. Within this class one finds black holes that are dual to superfluid phases which spontaneously break the  $U(1)$  symmetry, with  $s$ -wave [1–3],  $p$ -wave [4–8] and  $d$ -wave [9–11] order. In addition there are phases that spontaneously break some of the Poincaré symmetries of the boundary theory, including helical current phases [12, 13] and striped phases [14–18]. These latter solutions break parity and time reversal invariance, but the holographic charge density waves of [19] do not. Furthermore, it is possible to simultaneously break both the  $U(1)$  symmetry and the Poincaré symmetry as in the helical  $p$ -wave and  $(p + ip)$ -wave superconducting phases [20, 21]. A further investigation of this latter class of examples will be the focus of this paper.

As in [20, 21] we will study a model in  $D = 5$  space-time dimensions which couples the metric to an abelian gauge-field and a charged two-form. The two-form,  $C$ , has mass  $|m|$ , charge  $e$  and is dual to a self-dual tensor operator in a dual  $d = 4$  CFT with scaling dimension  $\Delta = 2 + |m|$ . The high temperature phase of the CFT with non-vanishing chemical potential is spatially homogeneous and isotropic and is described by the electrically charged AdS-RN planar black hole solution. It was shown in [20] that the AdS-RN black hole becomes unstable if  $e^2 > m^2/2$ . More precisely, it was shown that there are linearised perturbations of the charged two-form labelled by wave-number  $k$ , associated with both  $p$ -wave and  $(p + ip)$ -wave order, which become tachyonic below some critical temperature. The instabilities first appear for  $k \neq 0$  and moreover, since the linearised perturbations are governed by exactly the same ODE, the instabilities for the two types of order appear at the same critical temperature.

Some fully back-reacted  $p$ -wave black hole solutions for this model were constructed in [21] and here we will review and extend that work. We will also construct the first back-reacted  $(p + ip)$ -wave black holes for this model. It is natural to ask which of the two phases is thermodynamically preferred and how they compete<sup>1</sup>. For a different class of models, involving  $SU(2)$  gauge-fields, and for vanishing wave num-

---

<sup>1</sup>Some other holographic studies of competing orders appear in [22–30].

ber, it was shown that the  $p$ -wave order is preferred over the  $(p + ip)$ -wave order [5]. By contrast here we will see that depending on the parameters  $e, m$  both the helical  $p$ -wave and the  $(p + ip)$ -wave superfluid phases can be preferred and there can be first order transitions between them.

The  $p$ -wave black hole solutions of [21], and those that we construct here, are static and spatially homogenous with a helical, Bianchi  $VII_0$  symmetry. They appear in two-parameter families specified by the temperature,  $T$ , and the wave-number,  $k$ , which fixes the pitch (i.e. the periodicity) of the helical order to be  $2\pi/k$ . At fixed  $T$  the thermodynamically preferred black holes are determined by minimising the free energy density with respect to  $k$ . The numerical results in [21] indicated that this condition is equivalent to a simple constraint on the boundary data. Here we will directly prove this result, which also follows from the general results recently obtained in [31] concerning the thermodynamics of periodic black brane solutions. As in [21], we find that the pitch of the helix monotonically increases as the temperature is initially lowered away from the critical temperature. For certain values of  $e, m$  we find  $p$ -wave black holes which exhibit the phenomenon of pitch inversion:  $k$  starts off positive, decreases down to zero, changes sign and then increases in magnitude as the temperature is lowered. Such a phenomenon is seen<sup>2</sup>, for example, in some chiral nematic liquid crystals and helimagnets. In the zero temperature limit,  $T \rightarrow 0$ , the  $p$ -wave black holes approach zero entropy ground states. For  $k > 0$  we find an IR Bianchi  $VII_0$  scaling solution as already seen in [21] (of a very similar type to [32]). We also find a new type of zero entropy ground state with  $k = 0$  and an IR scaling symmetry, somewhat similar to some solutions constructed in [33]. Finally, when  $k < 0$  we find evidence that at extremely low temperatures the black holes approach  $AdS_5$  in the IR, perturbed by marginal and *relevant*  $k$ -dependent operators. This novel emergence of conformal symmetry in the IR is somewhat reminiscent of the recent work on periodic potentials in [34].

The  $(p + ip)$ -wave black hole solutions are also labelled by temperature  $T$  and a wave-number  $k$  associated with a direction we will label  $x_1$ . The solutions are stationary and preserve two translations, in the  $x_2, x_3$  directions, as well as translations in the  $x_1$  direction when combined with a local gauge transformation. In addition they preserve one rotation in the  $x_2, x_3$  plane. Unlike the  $p$ -wave black holes, the continuous symmetry for the  $(p + ip)$ -wave black holes is the same for both  $k = 0$  and  $k \neq 0$ . These black holes obey some novel Smarr formulae, consistent with the

---

<sup>2</sup>It is worth pointing out that such a phenomenon is not present in the black holes dual to helical current phases that were studied in [12, 13].

results of [31]. The one-parameter family of thermodynamically preferred black holes obtained by minimising the free-energy density with respect to  $k$ , are again specified by simple constraints on the boundary data as expected from [31]. In contrast to the  $p$ -wave case the stress tensor for the one-parameter family of  $(p+ip)$ -wave black holes is that of a spatially homogeneous and isotropic ideal fluid. In the  $T \rightarrow 0$  limit the entropy density of the  $(p+ip)$ -wave black holes goes to zero; we have not managed to extract from the numerics a simple statement about the ground states. However, we provide some evidence that for some black holes an emergent conformal symmetry again appears.

The plan of the rest of the paper is as follows. Section 2 introduces the  $D = 5$  gravity model that we study, as well as the  $p$ -wave and the  $(p+ip)$ -wave instabilities of the AdS-RN black hole. The back-reacted  $p$ -wave and  $(p+ip)$ -wave black holes are discussed in sections 3 and 4, respectively. In section 5 we compare the thermodynamics of the two competing orders and we briefly conclude in section 6. There is one appendix in which we provide a derivation of the Smarr formula for the  $(p+ip)$ -wave black holes.

## 2 The model

We consider a theory of gravity in  $D = 5$  space-time dimensions coupled to a gauge-field  $A$  and a complex two-form  $C$  with Lagrangian density given by the five-form

$$\mathcal{L} = (R + 12) * 1 - \frac{1}{2} * F \wedge F - \frac{1}{2} * C \wedge \bar{C} - \frac{i}{2m} C \wedge \bar{H}, \quad (2.1)$$

where the bar denotes complex conjugation. The field strengths are given by

$$F = dA, \quad H = dC + ieA \wedge C. \quad (2.2)$$

The corresponding equations of motion are given by

$$\begin{aligned} R_{\mu\nu} &= -4g_{\mu\nu} + \frac{1}{2} (F_{\mu}{}^{\rho} F_{\nu\rho} - \frac{1}{6} g_{\mu\nu} F_{\rho\sigma} F^{\rho\sigma}) + \frac{1}{2} (C_{(\mu}{}^{\rho} \bar{C}_{\nu)\rho} - \frac{1}{6} g_{\mu\nu} C_{\rho\sigma} \bar{C}^{\rho\sigma}), \\ d * F &= -\frac{e}{2m} C \wedge \bar{C}, \\ H &= -im * C. \end{aligned} \quad (2.3)$$

The equations of motion admit a unique  $AdS_5$  solution, with  $A = C = 0$ , which is dual to a class of CFTs labelled by the two-parameters  $e$  and  $m$ . The equations of motion also admit the electrically charged AdS-Reissner-Nordstrom black brane solution given by

$$ds^2 = -gdt^2 + g^{-1}dr^2 + r^2(dx_1^2 + dx_2^2 + dx_3^2), \quad A = adt, \quad (2.4)$$

with  $C = 0$  and

$$g = r^2 - \frac{r_+^4}{r^2} + \frac{\mu^2}{3} \left( \frac{r_+^4}{r^4} - \frac{r_+^2}{r^2} \right), \quad a = \mu \left( 1 - \frac{r_+^2}{r^2} \right). \quad (2.5)$$

The AdS-RN black hole has temperature  $T = (6r_+^2 - \mu^2)/6\pi r_+$  and describes the high temperature, spatially homogeneous and isotropic phase of the dual CFT when held at finite chemical potential  $\mu$  with respect to the global abelian symmetry.

It was shown in [20] that when  $e^2 > m^2/2$  these black holes are unstable<sup>3</sup> below a critical temperature corresponding to the formation of superconducting phases with either  $p$ -wave or  $(p + ip)$ -wave order. In the following sections we will construct fully back reacted black hole solutions corresponding to these two phases. For orientation let us first recall the linearised static perturbations, which only involve the charged two-form  $C$ , that appear at the onset of the instability.

For the  $p$ -wave instability the key part of the perturbation is given by

$$C = \dots + c_3(r) dx_1 \wedge [\sin(kx_1) dx_2 + \cos(kx_1) dx_3], \quad (2.6)$$

where the dots refer to terms that are determined from the function  $c_3(r)$  via the equations of motion. The boundary conditions that are imposed on  $c_3$  at the black hole horizon, located at  $r = r_+$ , and at the  $AdS$  boundary, located at  $r \rightarrow \infty$ , are, respectively,

$$\begin{aligned} c_3(r) &\sim c_{3+} + \mathcal{O}(r - r_+), \\ c_3(r) &\sim c_{c_3} r^{-|m|} + \dots, \quad r \rightarrow \infty. \end{aligned} \quad (2.7)$$

The former ensures regularity at the black hole horizon and the latter ensures that the symmetry breaking is spontaneous. Indeed the expectation value of the operator dual to  $C$ , with wave-number  $k$ , is proportional to  $c_{c_3}$ . Observe that when  $k = 0$ , the perturbation is given by  $C = \dots + c_3(r) dx_1 \wedge dx_3$ , corresponding to a  $p$ -wave vector order parameter pointing in the  $-x_2$  direction (after taking a three-dimensional Hodge dual). This is also called  $-p_{x_2}$  (or  $-p_y$ ) order. This is invariant under translations in three spatial directions and is also invariant under rotations in the  $(x_1, x_3)$  plane. When  $k \neq 0$  the order parameter rotates in the  $(x_2, x_3)$  plane as one moves along the  $x_1$  direction and there is a reduced helical (Bianchi VII<sub>0</sub>) symmetry. Indeed there are still translations in the  $x_2$  and  $x_3$  directions, while translations in the  $x_1$  direction should be supplemented by a rotation in the  $(x_2, x_3)$  plane.

---

<sup>3</sup>This was shown by analysing instabilities of the  $AdS_2 \times \mathbb{R}^3$  solution which arises as the near horizon limit of the  $T = 0$  AdS-RN black hole solution. In principle there could be additional instabilities which do not manifest themselves in this way.

For the  $(p + ip)$ -wave instability the key part of the perturbation is given by

$$C = \dots + e^{-ikx_1} ic_3(r) dx_1 \wedge (dx_2 - idx_3), \quad (2.8)$$

where the dots again refer to terms that are determined from  $c_3(r)$  from the equations of motion. The boundary conditions that are imposed on  $c_3$  are the same as in (2.7) with  $c_{c_3}$  fixing the expectation value of the operator dual to  $C$ , with wave-number  $k$ . When  $k = 0$ , we have a superposition of the order parameter for  $-p_{x_2}$  order and  $i$  times the order parameter for  $p_{x_3}$  order, so this is also called  $-p_{x_2} + ip_{x_3}$  order, or  $p + ip$  for short. When  $k \neq 0$  we see that this is invariant under three spatial translations as well as a combination of rotations in the  $(x_2, x_3)$  plane combined with a constant gauge transformation. When  $k \neq 0$  we have, essentially, the same continuous symmetry; the only difference is that the translation invariance in the  $x_1$  direction needs to be supplemented with a constant gauge transformation.

As shown in [20] the second order linear differential equation satisfied by  $c_3(r)$  is exactly the same for both the  $p$ -wave and the  $(p + ip)$ -wave linearised perturbation. We can use the linearity of the equation to set  $c_{3+} = 1$  in the boundary conditions given in (2.7). We then find that the critical temperature at which the static perturbations exist is a function of wave-number  $k$ , giving<sup>4</sup> the characteristic ‘‘bell curves’’ illustrated in figure 1 for  $m = 2$  and several values of  $e$ . For each value of  $k$  there will be two new branches of black hole solutions appearing at the temperature at which the static  $p$ -wave and  $(p + ip)$ -wave modes appear. This gives rise to two-parameter families of black hole solutions, labelled by  $k$  and  $T$ , for both the  $p$ -wave and the  $(p + ip)$ -wave cases. Constructing these solutions and finding the thermodynamically preferred solutions will be treated in subsequent sections. Observe that for fixed  $m = 2$ , increasing the charge  $e$  raises the critical temperature, as one expects for superconducting instabilities, and also broadens the width of the curves, as was previously seen in [20]. Note also that for  $m = 2$  and small enough  $e$ , (for example  $e = 1.7$ ) the bell curves do not cross the  $k = 0$  axis.

### 3 Helical $p$ -wave black holes

In this section we review the construction of [21], expanding on some of the details, and obtain some new results. The ansatz for the metric, gauge-field and two-form is

---

<sup>4</sup>For fixed  $(m, e)$ , there can be additional curves of zero modes appearing at lower temperatures as noticed in other contexts e.g. [5]. The zero modes corresponding to the higher critical temperature, as illustrated in figure 1, are the ones that drive the instability towards the black holes of interest. The other zero modes correspond to branches of black holes which are expected to be unstable.

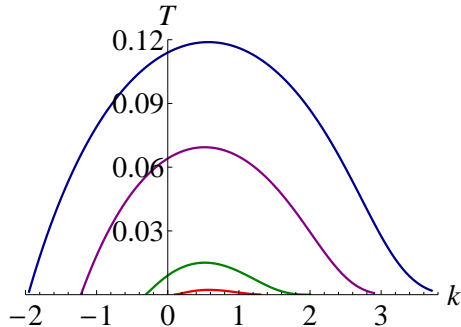


Figure 1: Plots of the critical temperature  $T$  versus wave-number  $k$  for the existence of normalisable, static perturbations of the two-form about the AdS-RN black hole solution, for both  $p$ -wave and  $(p + ip)$ -wave order. The plots are for  $m = 2$  and, from top to bottom  $e = 3.5$  (blue),  $e = 2.8$  (purple),  $e = 2$  (green) and  $e = 1.7$  (red). We have set the scale via  $\mu = 1$ .

given by

$$\begin{aligned}
 ds^2 &= -g f^2 dt^2 + g^{-1} dr^2 + h^2 \omega_1^2 + r^2 (e^{2\alpha} \omega_2^2 + e^{-2\alpha} \omega_3^2) , \\
 A &= a dt , \\
 C &= (i c_1 dt + c_2 dr) \wedge \omega_2 + c_3 \omega_1 \wedge \omega_3 ,
 \end{aligned} \tag{3.1}$$

where the one-forms  $\omega_i$  are the left-invariant one-form of the Bianchi type  $VII_0$  Lie algebra given by

$$\begin{aligned}
 \omega_1 &= dx_1 , \\
 \omega_2 &= \cos(kx_1) dx_2 - \sin(kx_1) dx_3 , \\
 \omega_3 &= \sin(kx_1) dx_2 + \cos(kx_1) dx_3 .
 \end{aligned} \tag{3.2}$$

The ansatz depends on eight function  $f$ ,  $g$ ,  $h$ ,  $\alpha$ ,  $c_i$  and  $a$  which are all functions of the radial coordinate,  $r$ , and the wave-number,  $k$ , is a constant. Notice that the ansatz is periodic in the  $x_1$  direction with period  $2\pi/k$ , a quantity also known as the pitch of the helix. We are principally interested in the case that all of the coordinates  $x_i$  are non-compact; the extension to the case of the coordinates  $x_i$  being compact is straightforward<sup>5</sup>. Notice that the ansatz is invariant under time translations associated with the Killing vector  $\partial_t$  and the spacetime is static. The ansatz is also spatially homogeneous with Bianchi  $VII_0$  symmetry corresponding to the Killing vectors  $\partial_{x_2}, \partial_{x_3}$ ,

<sup>5</sup>In the compact case only discrete values of  $k$  consistent with the fixed period of  $x_1$  are allowed. Furthermore, to obtain the thermodynamically preferred configurations, discussed below, one should minimise the free energy as opposed to the free energy density.

generating translations in the  $x_2, x_3$  directions, and  $\partial_{x_1} - k(x_2\partial_{x_3} - x_3\partial_{x_2})$ , generating a helical motion consisting of a simultaneous translation in the  $x_1$  direction with a rotation in  $(x_2, x_3)$  plane. The case of  $k = 0$  will be discussed below, where we will see the appearance of an extra continuous symmetry.

The equations of motion we are interested in are obtained by substituting the ansatz (3.1) into the  $D = 5$  equations of motion (2.3). They can also be obtained by substituting the ansatz (3.1) directly into the  $D = 5$  action (2.1) to obtain

$$\begin{aligned}
S = \int d^5x r^2 h f \left\{ -g'' - g' \left( \frac{3f'}{f} + \frac{2h'}{h} + \frac{4}{r} \right) + 12 \right. \\
- 2g \left[ \frac{f''}{f} + \frac{f'}{f} \left( \frac{2}{r} + \frac{h'}{h} \right) + \frac{h''}{h} + \frac{2h'}{rh} + \frac{1}{r^2} + \alpha'^2 \right] + \frac{a'^2}{2f^2} - \frac{2k^2}{h^2} \sinh(2\alpha)^2 \\
\left. - \frac{c_3^2}{2h^2r^2} e^{2\alpha} + \frac{c_1^2}{2f^2r^2g} e^{-2\alpha} - \frac{gc_2^2}{2r^2} e^{-2\alpha} \right\} \\
+ \frac{1}{2m} \int d^5x \left\{ c_1c_3' - c_3c_1' + 2eac_2c_3 + 2kc_1c_2 \right\}, \tag{3.3}
\end{aligned}$$

and then varying with respect to the eight functions, holding  $k$  fixed. We find that  $f$  and  $g$  satisfy first order differential equations and that  $h, \alpha, a$  and  $c_3$  satisfy second order equations with  $c_1$  and  $c_2$  determined via

$$\begin{aligned}
c_1 &= -\frac{e^{2\alpha}}{e^{4\alpha}k^2 + m^2h^2} (e^{2\alpha}keac_3 + mhfgc_3'), \\
c_2 &= \frac{1}{fg} \frac{e^{2\alpha}}{e^{4\alpha}k^2 + m^2h^2} (meahc_3 - e^{2\alpha}kfgc_3'). \tag{3.4}
\end{aligned}$$

One can substitute these back into the action (3.3) to obtain an action which will reproduce the equations of motion for  $f, g, h, \alpha, a$  and  $c_3$ . The ansatz, and hence the equations of motion, are invariant under the following three scaling symmetries:

$$\begin{aligned}
r &\rightarrow \lambda r, & (t, x_2, x_3) &\rightarrow \lambda^{-1}(t, x_2, x_3), & g &\rightarrow \lambda^2 g, & a &\rightarrow \lambda a, & c_3 &\rightarrow \lambda c_3; \\
x_1 &\rightarrow \lambda^{-1} x_1, & h &\rightarrow \lambda h, & k &\rightarrow \lambda k, & c_3 &\rightarrow \lambda c_3; \\
t &\rightarrow \lambda t, & f &\rightarrow \lambda^{-1} f, & a &\rightarrow \lambda^{-1} a; \tag{3.5}
\end{aligned}$$

where  $\lambda$  is a constant.

### 3.1 Asymptotic and near-horizon expansions

We now discuss the boundary conditions to be imposed for the helical  $p$ -wave black holes solutions. As  $r \rightarrow \infty$  we demand that we approach  $AdS_5$  with asymptotic

expansion

$$\begin{aligned}
g &= r^2 (1 - Mr^{-4} + \dots), & f &= f_0 (1 - c_h r^{-4} + \dots), \\
h &= r (1 + c_h r^{-4} + \dots), & \alpha &= c_\alpha r^{-4} + \dots, \\
a &= f_0 (\mu + qr^{-2} + \dots), & c_3 &= c_{c_3} r^{-|m|} + \dots,
\end{aligned} \tag{3.6}$$

which is specified by eight parameters  $M, f_0, c_h, c_\alpha, \mu, q, c_{c_3}$  and  $k$ . Notice that the boundary condition  $h \sim r$  implies that the wave-number  $k$  cannot be scaled away via (3.5). However, the scaling symmetries do allow us to set  $\mu = f_0 = 1$ , and we will do so later (it is helpful to keep them to discuss the thermodynamics). Observe that the fall-off of  $c_3$  is chosen so that the charged operator dual to the two-form  $C$  has no deformation but can acquire, *spontaneously*, an expectation value proportional to  $c_{c_3}$  which is spatially modulated in the  $x_1$  direction with period  $2\pi/k$ . The holographic interpretation of the other UV parameters will be given below.

We also demand that we have a regular black hole event horizon located at  $r = r_+$ . As  $r \rightarrow r_+$ , the functions have the analytic expansion

$$\begin{aligned}
g &= g_+(r - r_+) + \dots, & f &= f_+ + \dots, \\
h &= h_+ + \dots, & \alpha &= \alpha_+ + \dots, \\
a &= a_+(r - r_+) + \dots, & c_3 &= c_{3+} + \dots.
\end{aligned} \tag{3.7}$$

We find that the full IR expansion is fixed in terms of the six constants  $f_+, h_+, \alpha_+, a_+, c_{3+}$  and  $r_+$ . In particular, the coefficient  $g_+$  is fixed by these constants:

$$g_+ = r_+ \left( 4 - \frac{a_+^2}{6f_+^2} \right) - \frac{c_{3+}^2 e^{2\alpha_+}}{12r_+ h_+^2}. \tag{3.8}$$

The equations of motion give four second order differential equations for  $h, \alpha, a, c_3$  and two first order equations for  $g, f$  and hence a solution is specified by ten integrations constants. On the other hand we have fourteen parameters in the boundary conditions minus two for the scaling symmetries. We thus expect a two-parameter family of black hole solutions that can be specified by temperature  $T$  and wave number  $k$ .

## 3.2 Numerical solutions

We have numerically constructed these black holes and have summarised some of the results in figures 2 and 3, for  $m = 2$  and various values of  $e$  (note that black holes with  $m = 1.7$  and  $e = 1.88$  were constructed in [20]). Various aspects of these black

holes, including their thermodynamics and ground states, will be discussed in the following subsections. In figure 2 we display the two-parameter family of  $p$ -wave black holes, corresponding to the bell curves in figure 1, including the thermodynamically preferred branch obtained by minimising the free-energy density with respect to  $k$  at fixed  $T$ , as we discuss below. Note that all black holes have smaller free energy than the AdS-RN black hole and that the transition to the  $p$ -wave preferred branch is second order. In figure 3 we have plotted various physical quantities for the preferred branch for the representative case of  $m = 2$ ,  $e = 3.5$ ; other values of  $e$  are similar. We discuss the behaviour of solutions as  $T \rightarrow 0$  in section 3.7; in all cases it appears that the black holes approach zero entropy ground states with a behaviour consistent with an emergent scaling symmetry.

### 3.3 Thermodynamics

We analytically continue by setting  $t = -i\tau$ . Regularity of the solution at  $r = r_+$  is achieved by making  $\tau$  periodic with period  $\Delta\tau = 4\pi/(g_+f_+)$  corresponding to temperature  $T = (f_0\Delta\tau)^{-1}$ . Note that to ensure we get a real gauge-field and two-form field near  $r = r_+$  we should set  $a_+ = i\bar{a}_+$  and  $c_{1+} = i\bar{c}_{1+}$ . We can also read off the area of the event horizon and since we are working in units with  $16\pi G = 1$ , we deduce that entropy density is given by

$$s = 4\pi r_+^2 h_+. \quad (3.9)$$

We will consider the total Euclidean action,  $I_{Tot}$ , defined as

$$I_{Tot} = I + I_{ct}, \quad (3.10)$$

where  $I = -iS$  and the counter-term action is given by an integral on the boundary  $r \rightarrow \infty$ :

$$I_{ct} = \int d\tau d^3x \sqrt{-g_\infty} (-2K + 6 + \dots). \quad (3.11)$$

Here  $K = g^{\mu\nu} \nabla_\mu n_\nu$  is the trace of the extrinsic curvature of the boundary, where  $n^\mu$  is an outward pointing normal unit vector, and  $g_\infty$  is the determinant of the induced metric. The ellipsis refers to terms which will not be relevant for the ansatz and boundary conditions that we are considering. For our ansatz we have

$$I_{ct} = Vol_3 \Delta\tau \lim_{r \rightarrow \infty} r^2 h f g^{1/2} [6 - 2g^{1/2} (\frac{2}{r} + \frac{f'}{f} + \frac{h'}{h}) - g^{-1/2} g'], \quad (3.12)$$

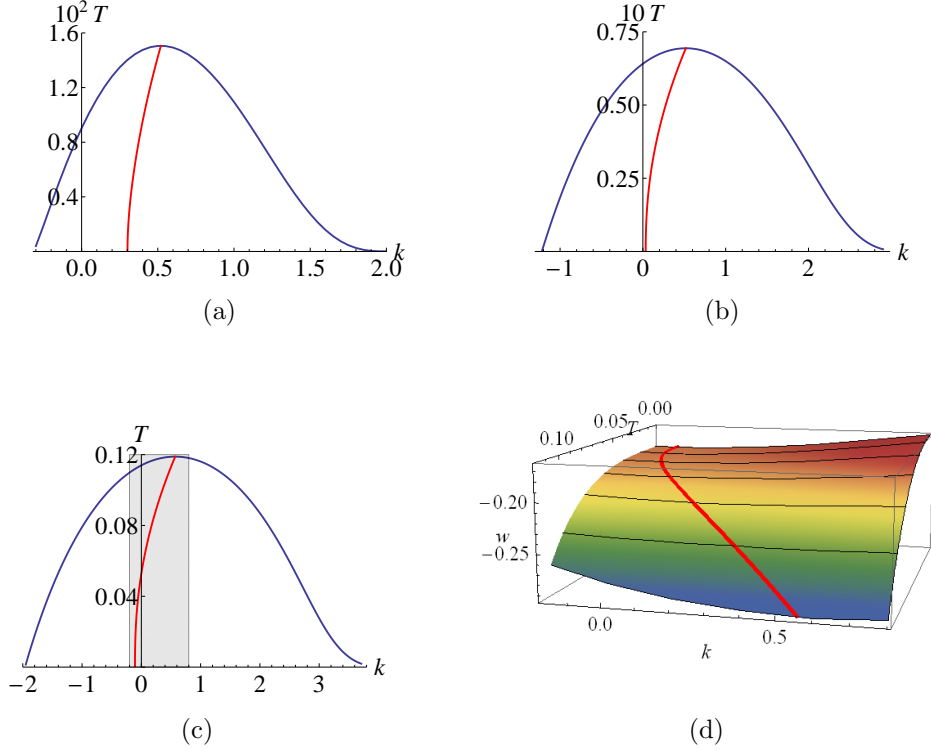


Figure 2:  $p$ -wave black holes for  $m = 2$  and  $e = 2$  (panel (a)),  $e = 2.8$  (panel (b)) and  $e = 3.5$  (panels (c) and (d)). Each point under the bell curve corresponds to a  $p$ -wave black hole at temperature  $T$  and wave-number  $k$ . All of these black holes have smaller free energy than the AdS-RN black hole at the same temperature. The red curve in each panel corresponds to the thermodynamically preferred branch of black holes that minimise the free energy density with respect to  $k$  at fixed  $T$ . In panel (d) we have plotted the free-energy density as a function of  $T$  and  $k$  for the representative case of  $e = 3.5$ ; the slice of  $k$ -values is represented by the grey shaded region in panel (c). For  $e = 2$  we see in panel (a) that the pitch ( $2\pi/k$ ) monotonically increases to a constant positive value at  $T = 0$ . For larger values of  $e$ , such as  $e = 3.5$  in panel (c), the black holes exhibit pitch inversion, with  $k = 0$  at some non-zero  $T$ . We have set  $\mu = 1$ .

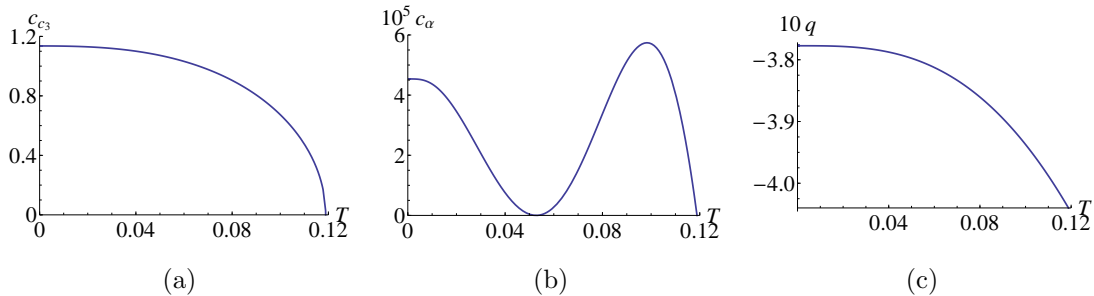


Figure 3: Properties of  $p$ -wave black holes for  $m = 2$  and  $e = 3.5$  as a function of  $T$  for the thermodynamically preferred branch (the red lines in figures 2(c) and 2(d)). Panel (a) plots  $c_{c3}$  which fixes the  $p$ -wave order parameter; panel (b) plots  $c_\alpha$  which fixes spatial modulation of the stress tensor - observe that it goes to zero at the temperature where the pitch inversion occurs; panel (c) plots  $q$  which fixes the charge density. Note that the thermodynamically preferred black holes have  $c_h = 0$ . We have set  $\mu = 1$ .

where  $Vol_3 = \int dx_1 dx_2 dx_3$ . We next point out two equivalent ways to write the bulk part of the Euclidean action on-shell:

$$\begin{aligned}
 I_{OS} &= Vol_3 \Delta\tau \int_{r_+}^{\infty} (2rghf)' , \\
 &= Vol_3 \Delta\tau \int_{r_+}^{\infty} \left( r^2 h f g' + 2r^2 h g f' - \frac{r^2 h a a'}{f} + \frac{c_1 c_3}{2m} \right)' , \quad (3.13)
 \end{aligned}$$

where  $c_1$  is given in (3.4). Notice that the first expression only receives contributions from the boundary at  $r \rightarrow \infty$  since  $g(r_+) = 0$ , while the second expression also receives contributions from  $r = r_+$ . We next define the free energy  $W = T[I_{Tot}]_{OS} \equiv w Vol_3$ . Using the UV and the IR expansions (3.6), (3.7) we obtain the following expression for the free energy density:

$$\begin{aligned}
 w &= -M , \\
 &= 3M + 8c_h + 2\mu q - sT , \quad (3.14)
 \end{aligned}$$

and hence the Smarr-type formula:

$$4M + 8c_h + 2\mu q - sT = 0 . \quad (3.15)$$

An on-shell variation of the total action  $[I_{Tot}]_{OS}$ , for fixed  $k$ , gives

$$[\delta I_{Tot}]_{OS} = Vol_3 \Delta\tau [\delta f_0 (3M + 8c_h + 2\mu q) + 2f_0 q \delta\mu] . \quad (3.16)$$

In this variation we are holding  $\Delta\tau$  fixed and hence  $\Delta\tau\delta f_0 = -T^{-2}\delta T$ . We thus deduce that  $w = w(T, \mu)$  and the first law

$$\delta w = -s\delta T + 2q\delta\mu. \quad (3.17)$$

We now compute the expectation value of the boundary stress-energy tensor. The relevant terms are given by [35]

$$\langle T_{\mu\nu} \rangle = \lim_{r \rightarrow \infty} r^2 [-2K_{\mu\nu} + 2(K - 3)g_{\infty\mu\nu} + \dots]. \quad (3.18)$$

Using the asymptotic expansion (3.6), we obtain, after setting  $f_0 = 1$ ,

$$\begin{aligned} \langle T_{tt} \rangle &= 3M + 8c_h, \\ \langle T_{x_1x_1} \rangle &= M + 8c_h, \\ \langle T_{x_2x_2} \rangle &= M + 8c_\alpha \cos(2kx_1), \\ \langle T_{x_3x_3} \rangle &= M - 8c_\alpha \cos(2kx_1), \\ \langle T_{x_2x_3} \rangle &= -8c_\alpha \sin(2kx_1). \end{aligned} \quad (3.19)$$

We easily see that this is traceless with respect to the flat boundary metric. We also note that defining the energy density  $\varepsilon = 3M + 8c_h$ , we can rewrite  $w = \varepsilon - sT + 2\mu q$  and the first law takes the form  $\delta\varepsilon = T\delta s - 2\mu\delta q$ .

The next step is to calculate the expectation value of the current. The relevant terms are given by

$$\langle J_\mu \rangle = - \lim_{r \rightarrow \infty} r^3 [F_{r\mu} + \dots], \quad (3.20)$$

where the ellipsis refers to terms that will not be relevant here. Using (3.6), we find that the only non-zero component is given by

$$\langle J_t \rangle = 2q, \quad (3.21)$$

where we have again set  $f_0 = 1$ . As expected,  $q$  fixes the charge density.

### 3.3.1 Variation of $w$ with respect to $k$

We have constructed two-parameter families of  $p$ -wave black hole solutions that can be labelled by temperature  $T$  and wave-number  $k$  (see figure 2(d)). For a given temperature we are interested in the solution labelled by  $k_{min}$  which minimises the free energy density (as in figures 2(a)-(c)). These black holes are specified by varying the action  $I_{Tot}$  with respect to  $k$  and setting it to zero on-shell. For the numerically constructed black holes of [21] it was shown that these solutions have  $c_h = 0$ . Here we

will directly prove this fact, which also follows from the general results for periodic black branes obtained in [31], as we will explain.

The variation of the Euclidean action  $I_{Tot}$  with respect to  $k$ , which only gets contributions from the bulk piece  $I$ , gives

$$k \partial_k I_{Tot} = Vol_3 \Delta\tau \int_{r_+}^{\infty} dr \left[ -\frac{k}{m} c_1 c_2 + \frac{4k^2 r^2 f}{h} \sinh^2(2\alpha) \right], \quad (3.22)$$

where  $c_1, c_2$  are given in (3.4). After imposing the equations of motion we find that the integrand can be rewritten as a total derivative leading to

$$[k \partial_k I_{Tot}]_{OS} = I_{OS} + Vol_3 \Delta\tau \int_{r_+}^{\infty} dr \left[ -2r^2 h' f g - \frac{1}{2} \frac{e^{2\alpha} h f g}{e^{4\alpha} k^2 + m^2 h^2} c_3 c_3' - \frac{k e}{2m} \frac{e^{4\alpha} a}{e^{4\alpha} k^2 + m^2 h^2} c_3^2 \right]', \quad (3.23)$$

where  $I_{OS}$  was given in (3.13). Evaluating the two terms on the right hand side by substituting the UV and the IR expansions (3.6), (3.7), we find that the divergent pieces cancel leading to the finite result  $[k \partial_k I_{Tot}]_{OS} = Vol_3 T^{-1} 8c_h$ . Hence, at constant  $T$  we have

$$k \partial_k w = 8c_h, \quad (3.24)$$

and hence the one-parameter family of thermodynamically preferred black holes satisfy the necessary condition

$$\partial_k w = 0 \quad \Rightarrow \quad c_h = 0, \quad (3.25)$$

We will see in section 3.4 that this is *not* a sufficient condition for picking out the preferred branch. The thermodynamically preferred black holes are labelled by the red lines in figure 2. Note that for this one-parameter family of black holes (labelled by the temperature) the stress tensor of the boundary CFT given in (3.19) is still spatially modulated in the  $(x_2, x_3)$  plane.

### 3.3.2 Connection with the results of [31]

A general analysis of the thermodynamics of periodic black branes was carried out in [31]. It was shown that several results can be immediately obtained from the boundary stress tensor  $T^{\mu\nu}$  and the current  $J^\mu$ . Specifically, in the present set up it

was shown<sup>6</sup> that

$$\begin{aligned}
w &= -Ts - \bar{J}^t \mu + \bar{T}^{tt}, \\
w &= -\bar{T}^{x_2 x_2} = -\bar{T}^{x_3 x_3} \\
\delta w &= -\bar{J}^t \delta \mu - s \delta T + \frac{\delta k}{k} (w + T^{x_1 x_1}),
\end{aligned} \tag{3.26}$$

where the bars refer to quantities averaged in the  $x_1$  direction;  $\bar{J}^t = (k/2\pi) \int_0^{2\pi/k} dx_1 J^t$  and  $\bar{T}^{x_i x_i} = (k/2\pi) \int_0^{2\pi/k} dx_1 T^{x_i x_i}$ . Note also that we have used the conservation of the stress tensor to deduce that  $T^{x_1 x_1}$  is constant. Using the expressions for the stress tensor and current given in (3.19), (3.20) and substituting into (3.26) we find that

$$\begin{aligned}
w &= -Ts + 2q\mu + 3M + 8c_h, \\
w &= -M, \\
\delta w &= 2q\delta\mu - s\delta T + \frac{\delta k}{k} (w + M + 8c_h).
\end{aligned} \tag{3.27}$$

We thus recover the two expressions for the action derived earlier (3.14) and hence the Smarr formula (3.15). We also obtain the first law given in (3.17), (3.24). In particular, for the case that  $x_1$  is non-compact, we should impose  $\delta w/\delta k = 0$  and we thus have  $c_h = 0$  for the thermodynamically preferred black holes and furthermore that  $T^{x_1 x_1} = \bar{T}^{x_2 x_2} = \bar{T}^{x_3 x_3}$  as also noted in [31].

### 3.4 Solutions with $k = 0$

For values of  $m, e$  where the bell curves cross the  $k = 0$  axis (see figures 1 and 2), there are  $p$ -wave black hole solutions with  $k = 0$ . These black holes are not thermodynamically preferred, except at the specific temperature at which the red branch of thermodynamically preferred solutions intersects the  $k = 0$  line, corresponding to pitch inversion, as in figure 2(c) for  $m = 2$  and  $e = 3.5$ . For  $m = 2$  and  $e \sim 2.9$ , the  $k = 0$  black hole is the  $T = 0$  ground state of the  $p$ -wave black holes. In this subsection we discuss the entire  $k = 0$  branch.

The black holes with  $k = 0$  are translationally invariant in the  $x_1$  direction. We can use the results of [31] to conclude<sup>7</sup> that for this branch there will be a Smarr

<sup>6</sup>Note that we have used the fact that there are no source terms for the two-form  $C$ .

<sup>7</sup> For these solutions we can define the free energy density in some finite interval  $x_1 \in [0, L]$  and then take the limit  $L \rightarrow \infty$ . The variation of the free energy density with respect to varying  $L$  is given by  $-(w + M + 8c_h)$  [31] and the translation invariance in the  $x_1$  direction implies that this vanishes.

formula which implies  $w + M + 8c_h = 0$ . Since we also have  $w = -M$  from (3.14) we deduce that  $c_h = 0$ . In addition, we have  $\bar{T}^{x_i x_i} = M = T^{x_1 x_1}$  for  $i = 2, 3$ . On the other hand from (3.19) we now have  $\bar{T}^{x_i x_i} = M + c_\alpha$  for  $i = 2, 3$  and hence we conclude that for the  $k = 0$  black holes we also have  $c_\alpha = 0$ .

By analysing the equations of motion near  $r \rightarrow \infty$  one can see that  $c_h = c_\alpha = 0$  implies that functionally we have  $h = r e^{-\alpha}$ . Indeed one can show that setting  $h = r e^{-\alpha}$  is a consistent truncation of the equations of motion corresponding to the following ansatz for the  $k = 0$   $p$ -wave black holes:

$$\begin{aligned} ds^2 &= -g f^2 dt^2 + g^{-1} dr^2 + r^2 e^{-2\alpha} (dx_1^2 + dx_3^2) + r^2 e^{2\alpha} dx_2^2, \\ A &= a dt, \\ C &= (i c_1 dt + c_2 dr) \wedge dx_2 + c_3 dx_1 \wedge dx_3, \end{aligned} \tag{3.28}$$

and now with

$$c_1 = -\frac{e^{3\alpha} f g c_3'}{m r}, \quad c_2 = \frac{e^{3\alpha} e a c_3}{m f g r}. \tag{3.29}$$

Notice that  $c_3$  in the two-form picks out the  $x_2$  direction as being preferred. The metric ansatz reflects this anisotropic structure, but the specific black hole solutions have  $c_\alpha = 0$  leading to an isotropic energy-momentum tensor (see (3.19)). We also note that these  $k = 0$  black holes have more symmetry than those with  $k \neq 0$ : the Bianchi VII<sub>0</sub> symmetry is replaced with three spatial translations as well as rotations in the  $(x_1, x_3)$  plane and this is related to the fact that  $h = r e^{-\alpha}$  is a consistent truncation of the equations of motion.

It is helpful at this point to address a potential confusion. We have argued that the thermodynamically preferred black holes which minimise the free energy with respect to  $k$  have  $c_h = 0$ . The converse is not true. For example, the  $k = 0$  branch of black holes has  $c_h = 0$  but they do not (in general) comprise an extrema of the free-energy density. It is illuminating to plot the behaviour of  $c_h$  against  $k$  for some representative temperatures, as in figure 4. It is also interesting to observe that from (3.22) we can conclude that at  $k = 0$  we have  $\partial_k w = -1/m \int_{r_+}^{\infty} dr c_1 c_2$ . In particular, we can establish that the  $k = 0$  solutions are unstable by obtaining a non-vanishing result for the integral for the  $k = 0$  branch of solutions. Furthermore, by taking a derivative of (3.24) with respect to  $k$ , we deduce that, with non-diverging  $\partial_k^2 w$ , this integral is given by  $8\partial_k c_h$  at  $k = 0$ .

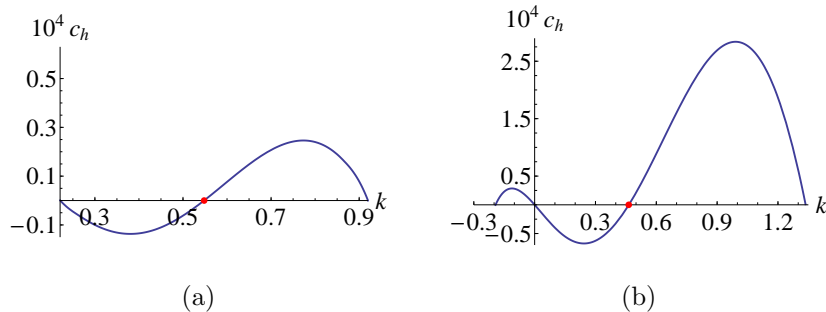


Figure 4: A plot of  $c_h$  versus  $k$  for  $p$ -wave black holes with  $m = 2$  and  $e = 3.5$  at temperature  $T = 0.117$  (panel (a)) and  $T = 0.11$  (panel (b)). The range of  $k$  plotted corresponds to the range of  $k$  in the bell curve in figure 2(c) for the two temperatures. In panel (a) we see that there is one zero of  $c_h$  in the interior, corresponding to the red branch, while in panel (b) there are two zeroes, one corresponding to the red branch (marked with the red dot) and the other to the  $k = 0$  branch. We have set the scale via  $\mu = 1$ .

### 3.5 Pitch inversion

In figure 2 we see that the value of  $k$  for the thermodynamically preferred black holes monotonically decreases as the temperature is lowered, for  $m = 2$  and various values of  $e$ . When  $m = 2$  and  $e = 2$ , for example,  $k$  decreases to a value  $k > 0$  at  $T = 0$ . As  $e$  is increased we observe the phenomena of pitch inversion. For example, when  $m = 2$  and  $e = 3.5$  the pitch ( $2\pi/k$ ) first increases, becoming infinite (i.e.  $k = 0$ ) at  $T \approx 0.053$  and then changes sign and decreases in magnitude leading to a value  $k < 0$  at  $T = 0$ . It is interesting to note that precisely at the pitch inversion temperature the symmetry of the black hole solutions is enhanced.

Notice that for  $m=2$  the numerics indicate that if  $e \lesssim 2.9$  then the preferred black holes hit a  $T = 0$  ground state with  $k > 0$ , while if  $e \gtrsim 2.9$  they hit a  $k < 0$  ground state. For the intermediate value<sup>8</sup>,  $e \sim 2.9$ , the ground state has  $k = 0$ . We will describe these ground states and their infrared scaling behaviour in the next subsections.

### 3.6 Scaling symmetry ground states with $k \neq 0$ and $k = 0$

In this subsection we present some solutions to the equations of motion with scaling symmetry. We also discuss the corresponding domain wall solutions which interpolate

<sup>8</sup>It is difficult, numerically, to extract the precise value of  $e$  at which this occurs.

between  $AdS_5$  in the UV and the scaling solutions in the IR which provide putative ground states for the  $p$ -wave black holes at  $T = 0$ .

There are scaling solutions with  $k \neq 0$  and Bianchi VII<sub>0</sub> symmetry that were first discussed in [21] (and are similar to those in [32]). We will see that these appear to correspond to the IR behaviour of the  $T = 0$   $p$ -wave black holes which have  $k > 0$  at  $T = 0$  (i.e.  $e \lesssim 2.9$ ). There are also scaling solutions with  $k = 0$  that are new and share some similarities to the scaling solutions discussed in [33]. These appear to correspond to the IR behaviour of the  $T = 0$   $p$ -wave black holes which have  $k = 0$  at  $T = 0$  (i.e.  $e \sim 2.9$ ). Interestingly, the  $p$ -wave black holes which have  $k < 0$  at  $T = 0$  (i.e.  $e \gtrsim 2.9$ ) appear to approach  $AdS_5$  in the IR. We will explain how the corresponding domain wall solutions can be constructed using  $k$ -dependent relevant perturbations in the IR.

### 3.6.1 Scaling solutions with $k \neq 0$ and Bianchi VII<sub>0</sub> symmetry

When  $k \neq 0$  the equations of motion admit scaling solutions of the form [21]

$$g = L^{-2}r^2, \quad f = \bar{f}_0 r^{z-1}, \quad h = kh_0, \quad \alpha = \alpha_0, \quad a = \bar{f}_0 a_0 r^z, \quad c_3 = kc_3^0 r, \quad (3.30)$$

where  $z, L, \bar{f}_0, h_0, \alpha_0, a_0$  and  $c_3^0$  are constants. For example, the metric for these solutions reads

$$ds^2 = -(\bar{f}_0^2 L^{-2})r^{2z} dt^2 + L^2 \frac{dr^2}{r^2} + (k^2 h_0^2) dx_1^2 + r^2 (e^{2\alpha_0} \omega_2^2 + e^{-2\alpha_0} \omega_3^2), \quad (3.31)$$

where  $\omega_i$  are the left invariant Bianchi VII<sub>0</sub> one-forms given in (3.2). By scaling  $t$  and  $x_1$  we can set  $\bar{f}_0 = k = 1$ . These fixed point solutions are invariant under the anisotropic scaling

$$r \rightarrow \lambda^{-1}r, \quad t \rightarrow \lambda^z t, \quad x_{2,3} \rightarrow \lambda x_{2,3}, \quad x_1 \rightarrow x_1. \quad (3.32)$$

After substituting into the equations of motion we obtain a system of algebraic equations which can be solved numerically. We find solutions provided  $e \gtrsim 1.13$  and we have displayed the values of  $z$  in figure 5. In particular, these fixed point solutions exist for all of the unstable AdS-RN black holes and hence can provide the IR limit of the zero temperature ground states of the  $p$ -wave black holes when  $k \neq 0$ . In fact this seems to be only true for the  $p$ -wave black holes with  $k > 0$  at  $T = 0$ .

To investigate the associated zero temperature domain wall solutions we need to

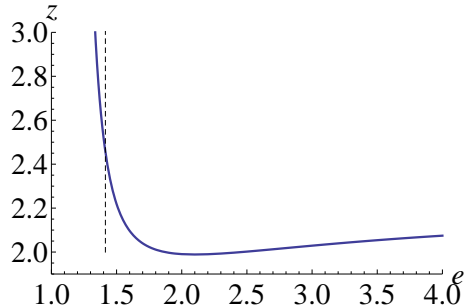


Figure 5: The scaling parameter  $z$  for helical fixed point solutions with  $k \neq 0$  of the form (3.30), (3.31) as a function of  $e$  with  $m = 2$  and  $e \gtrsim 1.13$ . The dashed vertical line is  $e = \sqrt{2}$  and when  $e > \sqrt{2}$  the AdS-RN black hole solution is unstable.

examine perturbations about the fixed point solution. We consider

$$\begin{aligned}
 g &= r^2 (L^{-2} + \lambda w_1 r^\delta), & f &= \bar{f}_0 r^{z-1} (1 + \lambda w_2 r^\delta), \\
 h &= k (h_0 + \lambda w_3 r^\delta), & \alpha &= \alpha_0 + \lambda w_4 r^\delta, \\
 a &= \bar{f}_0 a_0 r^z (1 + \lambda w_5 r^\delta), & c_3 &= k c_3^0 r (1 + \lambda w_6 r^\delta).
 \end{aligned} \tag{3.33}$$

After expanding the equations of motion at first order in  $\lambda$  we obtain a homogeneous linear system of equations  $\mathbf{E} \cdot \mathbf{w} = 0$  where  $\mathbf{E}$  is a  $6 \times 6$  matrix that depends on  $\delta$ . Demanding non-trivial solutions for  $\mathbf{w}$  we determine the values of  $\delta$  by solving the polynomial equation  $|\mathbf{E}| = 0$ . The solutions come in five pairs with the sum of each pair equal to  $-(2 + z)$ , as expected from a consideration of the scalar Laplacian for the metric (3.31). When  $m = 2$ ,  $e = 2$  the modes with non-negative real parts have  $\delta_1 = 0$ ,  $\delta_{2,3} \approx 0.83 \pm 1.01i$ ,  $\delta_4 \approx 0.94$  and  $\delta_5 \approx 3.12$ . In particular there is a pair related by complex conjugation<sup>9</sup>. For different values of  $e$  and  $m = 2$  this structure persists, with  $\delta_1 = 0$  and one complex-pair, except when  $1.24 \lesssim e \lesssim 1.31$  when all values of  $\delta$  are real; see figure 6.

To construct domain wall solutions with (3.30) as the far IR behaviour, one needs to shoot out using these five modes. Notice that the mode with  $\delta = 0$  corresponds to the constant  $\bar{f}_0$ . This leads to five (real) parameters in the IR. With the eight parameters mentioned for the UV discussed in (3.6) and two scaling symmetries from (3.5), we deduce that the domain wall solutions will be specified by a single parameter which we can take to be the wave-number  $k$ . Note that such domain walls were constructed in [21] for  $m = 1.7$  and  $e = 1.88$  (a case where all  $\delta$  are real). It would be interesting to determine whether or not these domain wall solutions exist

<sup>9</sup>Such complex scaling dimensions are analogous to those appearing in [36].

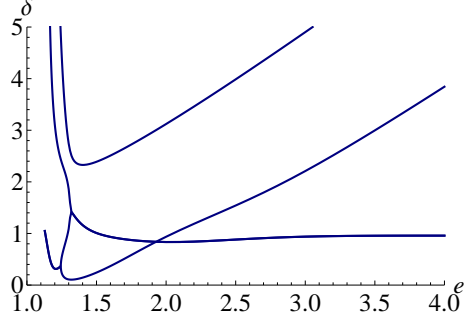


Figure 6: The scaling dimensions  $\delta$  with positive real parts, in the perturbations about the Bianchi VII<sub>0</sub> fixed point solution (3.30) with  $k \neq 0$  as a function of  $e$ , with  $m = 2$ . For  $1.24 \lesssim e \lesssim 1.31$  they are all real; for other values of  $e$  two are real and two form a complex pair, related by conjugation. There is also one mode with  $\delta = 0$ .

for all values of  $k \neq 0$ ; as we will discuss later, it is possible that they only exist for  $k > 0$ .

### 3.6.2 Scaling solutions with $k = 0$

When  $k = 0$  the equations of motion admit scaling solutions of the form

$$g = L^{-2}r^2, \quad f = \bar{f}_0 r^{z-1}, \quad h = \alpha_0^{-1} r^{1-\gamma}, \quad e^\alpha = \alpha_0 r^\gamma \quad a = \bar{f}_0 a_0 r^z, \quad c_3 = c_3^0 \alpha_0^{-2} r^{2(1-\gamma)}. \quad (3.34)$$

where  $z, L, \bar{f}_0, \gamma, \alpha_0, a_0$  and  $c_3^0$  are constants and we note that we are within the consistently truncated ansatz with  $h = r e^{-\alpha}$ . Explicitly, the full solution reads

$$\begin{aligned} ds^2 &= -(\bar{f}_0^2 L^{-2}) r^{2z} dt^2 + L^2 \frac{dr^2}{r^2} + \alpha_0^{-2} r^{2(1-\gamma)} (dx_1^2 + dx_3^2) + \alpha_0^2 r^{2(1+\gamma)} dx_2^2, \\ C &= \left(-i \frac{2(1-\gamma) \bar{f}_0 \alpha_0 c_3^0}{m L^2}\right) r^{z+1+\gamma} dt \wedge dx_2 + \left(\frac{e a_0 \alpha_0 c_3^0 L^2}{m}\right) r^\gamma dr \wedge dx_2 + (c_3^0 \alpha_0^{-2}) r^{2(1-\gamma)} dx_1 \wedge dx_3, \\ A &= (\bar{f}_0 a_0) r^z dt, \end{aligned} \quad (3.35)$$

By scaling  $t$  we can set  $\bar{f}_0 = 1$  and by suitably scaling  $x_1, x_3$  and  $x_2$  we can set  $\alpha_0 = 1$  too. These fixed point solutions are invariant under the anisotropic scaling

$$r \rightarrow \lambda^{-1} r, \quad t \rightarrow \lambda^z t, \quad x_{1,3} \rightarrow \lambda^{1-\gamma} x_{1,3}, \quad x_2 \rightarrow \lambda^{1+\gamma} x_2. \quad (3.36)$$

They are also translationally invariant in all three spatial directions and rotationally invariant in the  $x_1, x_3$  plane; they are somewhat similar to some solutions constructed in [33].

After substituting into the equations of motion we obtain a system of algebraic equations which can be solved numerically. We find solutions provided  $e \gtrsim 1.29$  and

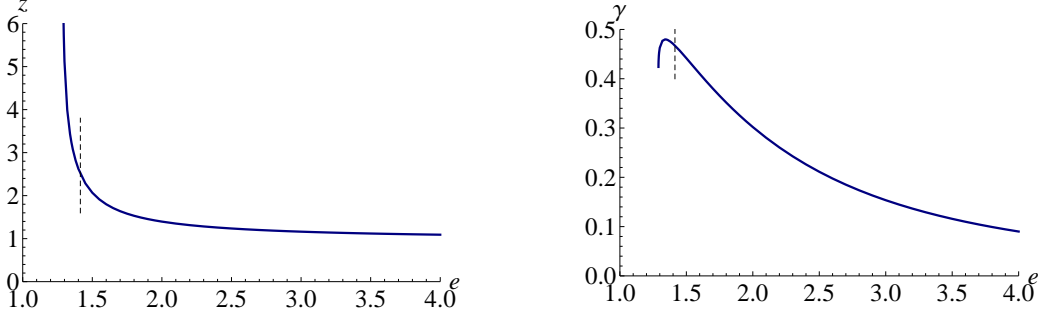


Figure 7: The scaling parameters  $z, \gamma$  for helical fixed point solutions with  $k = 0$  of the form (3.35) as a function of  $e$  with  $m = 2$  and  $e \gtrsim 1.29$ . The dashed vertical line is  $e = \sqrt{2}$  and when  $e > \sqrt{2}$  the AdS-RN black hole solution is unstable.

we have displayed the values of  $z$  and  $\gamma$  in figure 7. In particular we notice that these fixed point solutions exist for all of the unstable AdS-RN black holes and hence can provide the IR limit of the zero temperature ground states when  $k = 0$ .

To investigate zero temperature domain wall solutions we need to examine perturbations about the fixed point solution. We consider

$$\begin{aligned}
 g &= r^2 (L^{-2} + \lambda w_1 r^\delta), & f &= \bar{f}_0 r^{z-1} (1 + \lambda w_2 r^\delta), \\
 h &= r e^{-\alpha}, & e^\alpha &= \alpha_0 r^\gamma (1 + \lambda w_3 r^\delta), \\
 a &= \bar{f}_0 a_0 r^z (1 + \lambda w_4 r^\delta), & c_3 &= c_3^0 \alpha_0^{-2} r^{2(1-\gamma)} (1 + \lambda w_5 r^\delta).
 \end{aligned} \tag{3.37}$$

After expanding the equations of motion at first order in  $\lambda$  we obtain a homogeneous linear system of equations  $\mathbf{E} \cdot \mathbf{w} = 0$  where  $\mathbf{E}$  is a  $5 \times 5$  matrix that depends on  $\delta$ . Demanding non-trivial solutions for  $\mathbf{w}$  we determine the values of  $\delta$  by solving the polynomial equation  $|\mathbf{E}| = 0$ . The solutions come in four pairs with the sum of each element of a pair equal to  $-(3 + z - \gamma)$ , as expected. When  $m = 2$ ,  $e = 2$  the modes with non-negative real parts have  $\delta_{1,2} = 0$ , and  $\delta_{3,4} \approx 0.37 \pm 0.61i$ . In particular there is a pair related by complex conjugation. The two modes with  $\delta = 0$  are associated with the parameters  $\bar{f}_0$  and  $\alpha_0$  in (3.35). For different values of  $e$  and  $m = 2$  this structure persists, with  $\delta_{1,2} = 0$  and one complex-conjugate pair, except when  $e \lesssim 1.36$  when all values of  $\delta$  are real; see figure 8.

To construct domain wall solutions with (3.30) as the far IR behaviour, one needs to shoot out using these four modes in the IR. With the six parameters mentioned for the UV discussed in (3.6) (recall that for  $k =$  we have  $c_\alpha = c_h = 0$ ) and two scaling symmetries from (3.5), we can deduce that the domain wall solutions, if they exist, will be unique.

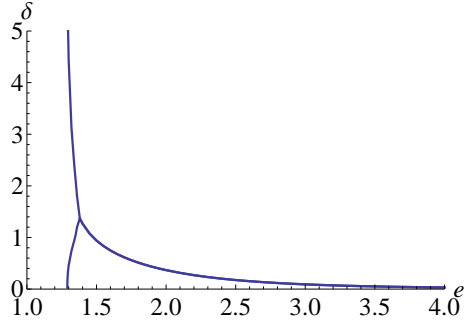


Figure 8: The scaling dimensions  $\delta$  with positive real parts, in the perturbations about the helical fixed point solution (3.35) with  $k = 0$  as a function of  $e$ , with  $m = 2$ . For  $e \lesssim 1.36$  they are both real and for  $e \gtrsim 1.36$ , they coalesce to form a complex conjugate pair. There are also two modes with  $\delta = 0$ .

### 3.6.3 Domain walls with $AdS_5$ in the IR

We now consider the possibility of constructing domain walls that interpolate between  $AdS_5$  in the UV and the *same*  $AdS_5$  in the IR. Since one usually shoots away from the UV and IR using relevant and irrelevant modes, respectively, and since we have the same  $AdS_5$  in the UV and the IR, one's first thought is that this won't be possible. On the other hand a construction was made in [37] using a massless complex scalar. In that work, the scalar was a constant in the IR and this provided mass for the gauge-field, transforming it into an irrelevant operator and enabling the construction of superconducting domain walls interpolating between the same  $AdS$  spacetime. Another construction in the context of  $p$ -wave superconductors with bulk  $SU(2)$  gauge fields appears in [38].

Here we will describe a new construction that instead exploits the  $k$  dependence of the relevant modes. Specifically, we have found that one can build up an expansion about the  $AdS_5$  spacetime as follows. We consider, as  $r \rightarrow 0$ ,

$$\begin{aligned} g &= r^2 + \delta g, & f &= \bar{f}_0 + \delta f, & h &= h_0 r + \delta h, \\ \alpha &= \delta \alpha, & c_3 &= \delta c_3, & a &= a_0 + \delta a, \end{aligned} \quad (3.38)$$

where  $\bar{f}_0, h_0$  and  $a_0$  are constants, associated with marginal deformations about the  $AdS_5$ . After substituting into the equations of motion, at first order in the perturbation we find that we need to solve second order linear ODEs for  $\delta \alpha$  and  $\delta c_3$ . Furthermore, we find that the following solution can be developed:

$$\delta \alpha = \alpha_0 \frac{e^{-2k/h_0 r}}{r^{3/2}} (1 + \mathcal{O}(r)), \quad \delta c_3 = c_3^0 \frac{e^{-kx/h_0 r}}{r^{1/2}} (1 + \mathcal{O}(r)), \quad (3.39)$$

where  $x = (1 - a_0^2 h_0^2 e^2 / \bar{f}_0^2 k^2)^{1/2}$  and  $\alpha_0, c_3^0$  are constants. Indeed going to second order in the perturbation (i.e. keeping terms with  $(c_3^0)^2, c_3^0 \alpha_0$  and  $\alpha_0^2$ ) we find

$$\begin{aligned}
g &= r^2 - \frac{(c_3^0)^2}{6h_0 k} x \frac{e^{-2kx/h_0 r}}{r^2} (1 + \mathcal{O}(r)) + \alpha_0^2 \frac{e^{-4k/h_0 r}}{r} (1 + \mathcal{O}(r)) \dots, \\
f &= \bar{f}_0 + \frac{(c_3^0)^2 \bar{f}_0 x}{12h_0 k} \frac{e^{-2kx/h_0 r}}{r^4} (1 + \mathcal{O}(r)) - \frac{\alpha_0^2 \bar{f}_0}{2} \frac{e^{-4k/h_0 r}}{r^3} (1 + \mathcal{O}(r)) \dots, \\
h &= h_0 r - \frac{(c_3^0)^2 a_0^2 h_0^3 e^2}{8\bar{f}_0^2 k^4 x^2} \frac{e^{-2kx/h_0 r}}{r^2} (1 + \mathcal{O}(r)) - \frac{\alpha_0^2 h_0}{2} \frac{e^{-4k/h_0 r}}{r^2} (1 + \mathcal{O}(r)) + \dots, \\
\alpha &= \alpha_0 \frac{e^{-2k/h_0 r}}{r^{3/2}} (1 + \mathcal{O}(r)) - \frac{(c_3^0)^2}{8k^2} \frac{e^{-2kx/h_0 r}}{r^3} (1 + \mathcal{O}(r)) + \dots, \\
c_3 &= c_3^0 \frac{e^{-kx/h_0 r}}{r^{1/2}} (1 + \mathcal{O}(r)) + \alpha_0 c_3^0 \frac{e^{-kx/h_0 r} e^{-2k/h_0 r}}{r^2} (1 + \mathcal{O}(r)) \dots, \\
a &= a_0 - \frac{(c_3^0)^2 \bar{f}_0 e}{4mk^2 x} \frac{e^{-2kx/h_0 r}}{r^2} (1 + \mathcal{O}(r)) + \dots.
\end{aligned} \tag{3.40}$$

Higher order corrections will involve higher powers of the exponential terms. The key aspect of this expansion is that the  $k$  dependent exponentials allow the corresponding terms to remain small as  $r \rightarrow 0$ . Notice that the  $k = 0$  limit of this expansion is not well-defined and this is consistent with the fact that it would not be possible to develop a  $k$  independent expansion in the IR associated with  $\delta\alpha$  and  $\delta c_3$  which are dual to relevant operators. Note also, that in contrast to [37], the function  $c_3$  governing the superconductivity is going to zero as  $r \rightarrow 0$ . Finally, we comment that a related expansion was, independently, recently used in a different context in [34].

Observe that this expansion has five IR parameters and so we expect that when combined with the eight UV parameters in (3.6) and the two scaling symmetries from (3.5), there will be a one-parameter family of domain wall solutions, which can be labelled by  $k$ .

### 3.7 The $T \rightarrow 0$ limit of the $p$ -wave black holes

For a given temperature  $T \neq 0$  the properties of the  $p$ -wave black holes depend continuously on  $k$ . For example, one can see this in the behaviour of the free-energy plot in figure 2(d). As  $T \rightarrow 0$ , all of the  $p$ -wave black holes appear to approach zero entropy ground states,  $s \rightarrow 0$ . However, the precise domain wall solutions that the black holes approach at  $T = 0$  depends on the sign of  $k$ , as we shall discuss. We note at the outset that in many cases the  $T \rightarrow 0$  behaviour only manifests itself at extremely low temperatures, which becomes very challenging to analyse numerically. The main strategy is to seek evidence that the entropy density scales with temperature

consistent with the scaling expected from a domain wall solution that hits a scaling solution in the far IR.

### 3.7.1 $k > 0$

For  $m = 1.7$  and  $e = 1.88$  it was shown in [21] that at  $T = 0$  the black holes with  $k > 0$  approach domain wall solutions which in the far IR approach scaling solutions with a Bianchi VII<sub>0</sub> symmetry (3.30). More precisely this was shown for the preferred branch of black holes, which had  $k > 0$  at  $T = 0$ , and it was also shown for black holes with slightly smaller and also larger values of  $k$ . In particular, explicit domain wall solutions were constructed in detail for these values of  $k$  but smaller values of  $k$ , including  $k \leq 0$ , were not studied.

For  $m = 2$  we again seem to find that for  $k > 0$  the black holes approach similar domain wall solutions with the Bianchi VII<sub>0</sub> fixed points (3.30) in the IR. Amongst other things, we have checked for the thermodynamically preferred branch black holes with  $e = 2$ , which have  $k = 0.30$  at  $T = 0$ , that the temperature dependence of the entropy has the appropriate scaling behaviour. Explicitly, if the black hole solutions approach the fixed points (3.30) in the IR, then a simple argument based on dimensional analysis (e.g. see [39]) shows that the entropy density should obey the scaling

$$s \propto T^{2/z}, \quad (3.41)$$

where the factor of two arises because only two of the spatial directions are involved in the scaling (3.32). For  $e = 2$  the appropriate value of  $z$  is given by  $z \sim 1.99$  (see figure 5). We have plotted our results in figure 9(a), and we note that we went down to temperatures of the order  $3 \times 10^{-8}$ .

### 3.7.2 $k = 0$

If the  $T \rightarrow 0$  black hole solutions approach  $k = 0$  domain walls with fixed points (3.35) in the IR, then dimensional analysis implies that the entropy density should behave like

$$s \propto T^{(3-\gamma)/z}. \quad (3.42)$$

For  $m = 2$  and  $e = 2$  we have found that the  $k = 0$  branch of black holes (which is not thermodynamically preferred) does in fact approach such scaling behaviour, as illustrated in figure 9(b). For this case the scaling behaviour again starts to manifest itself at very low temperatures.

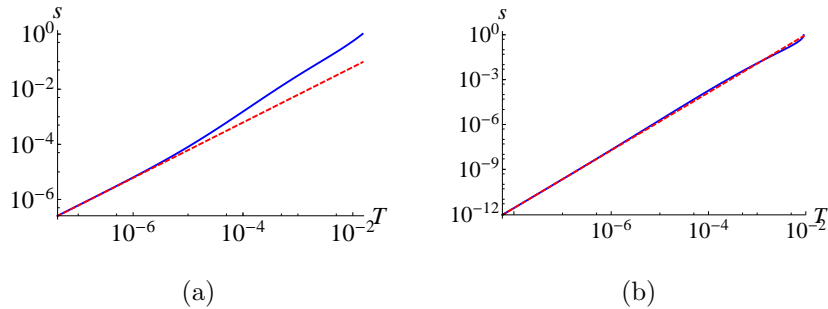


Figure 9: The low temperature behaviour of the entropy density  $s$  for the  $p$ -wave black holes for  $m = 2$  and  $e = 2$ . The blue line in panel (a) is for the thermodynamically preferred branch (the red line in figure 2a). It is consistent with the solutions approaching  $k > 0$  domain walls with Bianchi VII<sub>0</sub> fixed points in the IR (3.30) with  $s \propto T^{2/z}$  and  $z = 1.99$  (marked by the red dashed line). The blue line in panel (b) is for the *non-preferred*  $k = 0$  branch, consistent with the solutions approaching the scaling behaviour  $s \propto T^{(3-\gamma)/z}$  and  $z \sim 1.40$ ,  $\gamma \sim 0.0302$  associated with the scaling solution (3.35) (marked by the red dashed line). We have set  $\mu = 1$ .

### 3.7.3 $k < 0$

The  $T \rightarrow 0$  limits of the  $p$ -wave black holes with  $k < 0$  are the most difficult to analyse numerically. Nevertheless, our analysis of the behaviour of the functions near the horizon indicate that the black holes approach the  $AdS_5$  vacuum in the far IR, but the temperatures are extremely low. Indeed we have constructed black holes with temperatures of the order  $10^{-8}$  where some evidence of an  $AdS_5$  region appears to be building up near the black hole horizon. However, to get a conclusive picture one needs to go to even lower temperatures and this will be left for future work. The fact that we have provided evidence that there are appropriate domain wall solutions, using the expansion (3.40), lends support to the conclusion that an  $AdS_5$  appears in the far IR at  $T = 0$ .

### 3.7.4 Summary

Our results indicate the following picture for the  $T \rightarrow 0$  limits of the  $p$ -wave black holes. For  $k > 0$  they approach domain walls with Bianchi VII<sub>0</sub> scaling in the IR. For  $k = 0$  they approach domain walls with anisotropic scaling (3.35) in the IR. For  $k < 0$  they approach  $AdS_5$  in the IR.

It seems reasonable to conjecture that the domain walls with Bianchi VII<sub>0</sub> fixed

points in the IR in fact only exist for  $k > 0$  and similarly the domain walls with  $AdS_5$  in the IR only exist for  $k < 0$ . It will be interesting to investigate this further.

### 3.7.5 $\partial_T k = 0$ as $T \rightarrow 0$

A feature of the thermodynamically preferred red branches in figure 2, is that  $\partial_T k = 0$  as  $T \rightarrow 0$ . To conclude this section we explain this fact using the following simple argument. The free energy density  $w$  is a function of  $T, k$  and  $\mu$ . However, we are interested in holding  $\mu$  fixed and indeed we have set  $\mu = 1$  in our plots. The thermodynamically preferred black hole solutions satisfy  $\partial_k w = 0$  at fixed  $T$  (giving the condition  $c_h = 0$ ) and this specifies  $k = k(T)$  along this branch. Thus, along this branch we compute

$$\begin{aligned} 0 &= \frac{d}{dT}(\partial_k w) = \partial_{Tk}^2 w + \partial_k^2 w \partial_T k, \\ &= -\partial_k s + \partial_k^2 w \partial_T k. \end{aligned} \tag{3.43}$$

Since the thermodynamically preferred branch minimises the free energy we have (generically)  $\partial_k^2 w > 0$ . As  $T \rightarrow 0$  if the preferred solutions have  $\partial_k s = 0$ , for example if  $s \rightarrow 0$  in some open subset as we have for the  $p$ -wave black hole solutions, then we can conclude that  $\partial_T k = 0$  as  $T \rightarrow 0$ .

Clearly this argument applies more generally and indeed the behaviour  $\partial_T k = 0$  as  $T \rightarrow 0$  can be observed for the preferred branch of striped black holes constructed in [15–18, 40] (see figure 4 of [18]). We also note that the argument can be easily extended to black holes that are spatially modulated in more than one direction.

## 4 $(p + ip)$ -wave black holes

The ansatz we shall consider for the black holes describing holographic  $(p + ip)$ -wave superconductors is given by

$$\begin{aligned} ds^2 &= -gf^2 dt^2 + g^{-1} dr^2 + h^2(dx_1 + Qdt)^2 + r^2(dx_2^2 + dx_3^2), \\ A &= adt + bdx_1, \\ C &= e^{-ikx_1}(ic_1 dt + c_2 dr + ic_3 dx_1) \wedge (dx_2 - idx_3), \end{aligned} \tag{4.1}$$

where  $f, g, h, Q, a, b$  and  $c_i$  are nine functions of the radial coordinate  $r$  and  $k$  is a constant corresponding to the wave-number of the  $(p + ip)$ -wave order. The ansatz is invariant under time translations and when  $Q \neq 0$  the spacetime is stationary

but not static. The ansatz is invariant under translations in the  $x_2, x_3$  directions and also in the  $x_1$  direction when combined with a constant gauge transformation:  $x_1 \rightarrow x_1 + c$ ,  $C \rightarrow e^{ikc}C$ . The ansatz is invariant under rotations in the  $(x_2, x_3)$ -plane when combined with a gauge transformation or, when  $k \neq 0$ , a translation in the  $x_1$  direction. Observe that a gauge transformation can be used to eliminate the phase  $e^{ikx_1}$  appearing in  $C$  by making the shift  $b \rightarrow b - k/e$ . We will return to this point later.

The equations of motion we are interested in are obtained by substituting the ansatz (4.1) into (2.3). They can also be obtained by substituting the ansatz (4.1) directly into the action (2.1) to obtain

$$\begin{aligned}
S = \int d^5x r^2 h f \left\{ -g'' - g' \left( \frac{3f'}{f} + \frac{2h'}{h} + \frac{4}{r} \right) + 12 + \frac{h^2 Q'^2}{2f^2} \right. \\
- 2g \left[ \frac{f''}{f} + \frac{f'}{f} \left( \frac{2}{r} + \frac{h'}{h} \right) + \frac{h''}{h} + \frac{2h'}{rh} + \frac{1}{r^2} \right] + \frac{a'^2}{2f^2} - \frac{1}{2} \left( \frac{g}{h^2} - \frac{Q^2}{f^2} \right) b'^2 - \frac{Qa'b'}{f^2} \\
+ \frac{c_1^2}{r^2 f^2 g} - \frac{g c_2^2}{r^2} + \frac{1}{r^2} \left( \frac{Q^2}{f^2 g} - \frac{1}{h^2} \right) c_3^2 - \frac{2Qc_1 c_3}{r^2 f^2 g} \left. \right\} \\
+ \frac{1}{m} \int d^5x \left\{ c_1 c_3' - c_3 c_1' + 2e(ac_2 c_3 - bc_1 c_2) + 2kc_1 c_2 \right\}, \tag{4.2}
\end{aligned}$$

and then varying with respect to the nine functions, holding  $k$  fixed. We find that  $f$  and  $g$  satisfy first order differential equations and that  $h, Q, b, a$  and  $c_3$  satisfy second order equations with  $c_1$  and  $c_2$  completely determined in terms of  $c_3$  via

$$\begin{aligned}
c_1 &= \frac{[ea(eb - k) + m^2 h^2 Q]c_3 - mhfgc_3'}{m^2 h^2 + (eb - k)^2}, \\
c_2 &= \frac{[ea - Q(eb - k)]mhc_3 + fg(eb - k)c_3'}{fg[m^2 h^2 + (eb - k)^2]}. \tag{4.3}
\end{aligned}$$

We observe that our ansatz, and hence the equations of motion, are left invariant under the following three scaling symmetries:

$$\begin{aligned}
r &\rightarrow \lambda r, & (t, x_2, x_3) &\rightarrow \lambda^{-1}(t, x_2, x_3), & g &\rightarrow \lambda^2 g, & Q &\rightarrow \lambda Q, & a &\rightarrow \lambda a, & c_3 &\rightarrow \lambda c_3; \\
x_1 &\rightarrow \lambda^{-1} x_1, & h &\rightarrow \lambda h, & Q &\rightarrow \lambda^{-1} Q, & k &\rightarrow \lambda k, & b &\rightarrow \lambda b, & c_3 &\rightarrow \lambda c_3; \\
t &\rightarrow \lambda t, & f &\rightarrow \lambda^{-1} f, & a &\rightarrow \lambda^{-1} a, & Q &\rightarrow \lambda^{-1} Q; \tag{4.4}
\end{aligned}$$

where  $\lambda$  is a constant.

## 4.1 Asymptotic and near-horizon expansions

We will be interested in black hole solutions that asymptotically approach  $AdS_5$  in the UV and are dual to  $d = 4$  phases where the symmetry breaking is spontaneously generated. By analysing the equations of motion we can construct the following asymptotic expansion as  $r \rightarrow \infty$ :

$$\begin{aligned}
 g &= r^2(1 - Mr^{-4} + \dots), & f &= f_0(1 - c_h r^{-4} + \dots), \\
 h &= r(1 + c_h r^{-4} + \dots), & Q &= c_Q r^{-4} + \dots, \\
 a &= f_0(\mu + q r^{-2} + \dots), & b &= c_b r^{-2} + \dots, \\
 c_3 &= c_{c_3} r^{-|m|} + \dots.
 \end{aligned} \tag{4.5}$$

At a convenient juncture we will use the symmetries (4.4) to set  $f_0 = \mu = 1$ . The UV data is then specified by seven parameters  $M, c_h, c_Q, q, c_b, c_{c_3}$  and  $k$ . Note that we have fixed the asymptotic fall-off of  $h$  in (4.5) so we can no longer use (4.4) to scale  $k$ . The fall-off of  $c_{c_3}$  and  $b$  is appropriate for the spontaneous appearance of the  $(p + ip)$ -wave order, labelled by wave-number  $k$ . In particular, the fall-off of  $b$  corresponds to the absence of a source for the global  $U(1)$  symmetry in the boundary field theory. Observe, however, that if we implement the gauge transformation mentioned above to eliminate the phase  $e^{-ikx_1}$  appearing in the two-form  $C$ , then we should instead impose the UV boundary condition  $b = -k/e + c_b r^{-2}$ . The holographic interpretation of the other parameters appearing in the ansatz will become clear when we derive the holographic stress tensor and current, below.

At the black hole horizon, located at  $r = r_+$ , the functions have the analytic expansion

$$\begin{aligned}
 g &= g_+(r - r_+) + \dots, & f &= f_+ + \dots, \\
 h &= h_+ + \dots, & Q &= Q_+(r - r_+) + \dots, \\
 a &= a_+(r - r_+) + \dots, & b &= b_+ + \dots, \\
 c_3 &= c_{3+} + \dots.
 \end{aligned} \tag{4.6}$$

Regularity of the metric at the black hole horizon can easily be seen by using the in-going Eddington-Finkelstein coordinates  $v, r$  where  $v \approx t + (g_+ f_+)^{-1} \ln(r - r_+)$ . The full IR expansion is fixed in terms of the seven constants  $f_+, h_+, Q_+, a_+, b_+, c_{3+}$  and  $r_+$ . In particular, the coefficient  $g_+$  is fixed by these constants:

$$g_+ = r_+ \left( 4 - \frac{a_+^2}{6f_+^2} \right) - \frac{c_{3+}^2}{6r_+ h_+^2}. \tag{4.7}$$

After fixing the symmetries (4.4), we have seven UV parameters and seven IR parameters. We have two first order differential equations and five which are second order, so a solution is fixed by twelve integration constants. Thus, generically, we expect a two-parameter family black hole solutions, which we will label by the wave-number,  $k$ , and temperature,  $T$ .

## 4.2 Numerical solutions

We have numerically constructed these black holes for  $m = 2$  and various values of  $e$ , and we have summarised some of the results in figures 10 and 11. Some properties of these black holes, including their thermodynamics, will be discussed in the following subsections. In figure 10 we display the two-parameter family of  $(p + ip)$ -wave black holes, corresponding to the bell curves in figure 1, including the thermodynamically preferred branches obtained by minimising the free-energy density with respect to  $k$  at fixed  $T$ , as we discuss below. Note that all black holes have smaller free energy than the AdS-RN black hole and that the transition to the  $(p + ip)$ -wave preferred branch is second order. In figure 11 we have plotted various physical quantities for the preferred branch for the representative case of  $m = 2$ ,  $e = 3.5$ ; other values of  $e$  are similar. We will discuss the behaviour of the solutions as  $T \rightarrow 0$  in section 4.4 below, where we will see that the black holes have zero entropy ground states.

It appears from the figures that the thermodynamically preferred black holes do not cross the  $k = 0$  axis, except possibly at  $T = 0$ . However, for the case  $e = 3.5$  the detailed numerics show that the  $k = 0$  axis is crossed at temperatures of the order  $T \sim 0.015$  and we expect this phenomenon to persist for larger values of  $e$ .

## 4.3 Thermodynamics

We analytically continue by setting  $t = -i\tau$ . Near  $r = r_+$ , the Euclidean solution takes the approximate form

$$\begin{aligned}
 ds_E^2 &\approx g_+ f_+^2 (r - r_+) d\tau^2 + \frac{dr^2}{g_+(r - r_+)} + h_+^2 (dx_1 + \bar{Q}_+(r - r_+) d\tau)^2 + r_+^2 (dx_2^2 + dx_3^2), \\
 A &\approx \bar{a}_+(r - r_+) d\tau + b_+ dx_1, \\
 C &\approx e^{-ikx_1} (i\bar{c}_1 d\tau + c_{2+} dr + ic_{3+} dx_1) \wedge (dx_2 - idx_3),
 \end{aligned} \tag{4.8}$$

where we have defined  $Q_+ = i\bar{Q}_+$ ,  $a_+ = i\bar{a}_+$  and  $c_{1+} = ic_{1+}$  so that the metric, gauge-field and two-form are real. Regularity of the solution at  $r = r_+$  is easily seen by making the coordinate change  $\rho = 2g_+^{-1/2}(r - r_+)^{1/2}$  and making  $\tau$  periodic

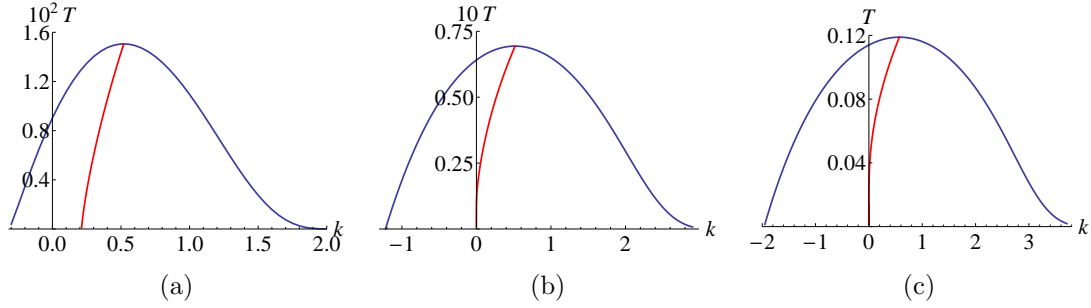


Figure 10:  $(p + ip)$ -wave black holes for  $m = 2$  and  $e = 2$  (panel (a)),  $e = 2.8$  (panel (b)) and  $e = 3.5$  (panel (c)). Each point under the bell curve corresponds to a  $(p + ip)$ -wave black hole at temperature  $T$  and wave-number  $k$ . All of these black holes have smaller free energy than the AdS-RN black hole at the same temperature. The red curve in each figure corresponds to the thermodynamically preferred branch of black holes that minimise the free energy density with respect to  $k$  at fixed  $T$ . For  $e = 3.5$  the  $k = 0$  axis is crossed by the red line at  $T \sim 0.015$ . We have set  $\mu = 1$ .

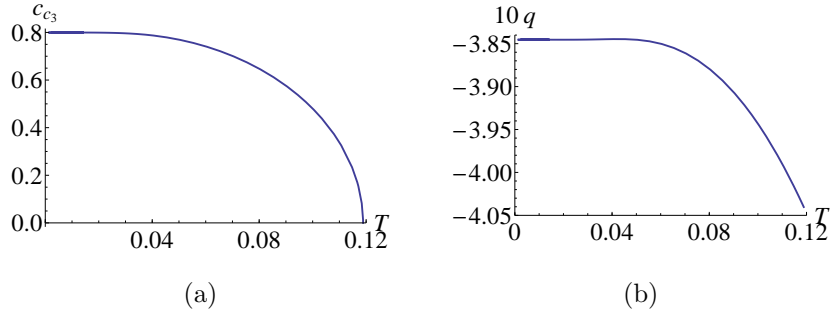


Figure 11: Properties of  $(p + ip)$ -wave black holes for  $m = 2$  and  $e = 3.5$  as a function of  $T$  for the thermodynamically preferred branch (the red line in figure 2(c)). Panel (a) plots  $c_{c_3}$  which fixes the  $(p + ip)$ -wave order parameter and panel (b) plots  $q$  which fixes the charge density. Note that these black holes have  $c_b = c_Q = c_h = 0$  and the entropy density is displayed in figure 12. We have set  $\mu = 1$ .

with period  $\Delta\tau = 4\pi/(g_+f_+)$  corresponding to temperature  $T = (f_0\Delta\tau)^{-1}$ . We can also read off the area of the event horizon and since we are working in units with  $16\pi G = 1$ , we deduce that entropy density is given by

$$s = 4\pi r^2 h_+. \quad (4.9)$$

The total Euclidean action,  $I_{Tot} = I + I_{ct}$  where  $I = -iS$  and the counter-term action  $I_{ct}$  is given in (3.11). In fact the expression (3.12) for the  $p$ -wave ansatz is also valid for the  $(p + ip)$ -wave ansatz. There are two equivalent ways to write the bulk part of the Euclidean action on-shell:

$$\begin{aligned} I_{OS} &= Vol_3 \Delta\tau \int_{r_+}^{\infty} (2rghf)' , \\ &= Vol_3 \Delta\tau \int_{r_+}^{\infty} \left( r^2 h f g' + 2r^2 h g f' + r^2 \frac{ha}{f} (Qb' - a') - \frac{r^2 h^3}{f} Q Q' \right. \\ &\quad \left. + c_3^2 \frac{-eka + m^2 h^2 Q + e^2 ab}{m[m^2 h^2 + (eb - k)^2]} - c_3 c_3' \frac{fgh}{[m^2 h^2 + (eb - k)^2]} \right)'. \end{aligned} \quad (4.10)$$

Notice that the first expression only receives contributions from the boundary at  $r \rightarrow \infty$  since  $g(r_+) = Q(r_+) = a(r_+) = 0$ , while the second expression also receives contributions from  $r = r_+$ . The free energy is defined by  $W = T[I_{Tot}]_{OS} \equiv w Vol_3$ . Using the UV and the IR expansions (4.5), (4.6) we obtain the following expression for the free-energy density

$$w = -M, \quad (4.11)$$

as well as the Smarr formula:

$$4M + 8c_h + 2\mu q - sT = 0. \quad (4.12)$$

Interestingly there are two further Smarr-type formulae that all of the  $(p + ip)$ -wave black holes satisfy, given by

$$\begin{aligned} 4c_h - \frac{k}{e} c_b &= 0, \\ 2c_Q + c_b \mu &= 0. \end{aligned} \quad (4.13)$$

A direct derivation is presented in appendix A. We can also obtain them using the results of [31], as we discuss below.

A variation of the total on-shell action  $[I_{Tot}]_{OS}$ , for fixed  $k$ , gives

$$[\delta I_{Tot}]_{OS} = Vol_3 \Delta\tau [\delta f_0 (3M + 8c_h + 2\mu q) + 2f_0 q \delta\mu]. \quad (4.14)$$

In this variation we are holding  $\Delta\tau$  fixed and hence  $\Delta\tau\delta f_0 = -T^{-2}\delta T$ . We next define the free energy  $W$ , and a corresponding density  $w$ , for the grand canonical ensemble via  $W = T[I_{Tot}]_{OS} = wVol_3$ . We deduce that  $w = w(T, \mu)$  with the first law given by

$$\delta w = -s\delta T + 2q\delta\mu. \quad (4.15)$$

We now compute the expectation value of the boundary stress-energy tensor. The relevant terms are again given by (3.18) and using the asymptotic expansion (4.5), we obtain

$$\begin{aligned} \langle T_{tt} \rangle &= 3M + 8c_h, \\ \langle T_{tx_1} \rangle &= 4c_Q, \\ \langle T_{x_1x_1} \rangle &= M + 8c_h, \\ \langle T_{x_2x_2} \rangle &= M, \\ \langle T_{x_3x_3} \rangle &= M, \end{aligned} \quad (4.16)$$

where we have set  $f_0 = 1$ . One can easily check that this is traceless with respect to the flat boundary metric. We also notice that unlike the  $p$ -wave black holes, there is no spatial modulation of the stress tensor while on the other hand there is, in general, momentum density in the  $x_1$  direction. Defining the energy density  $\varepsilon = 3M + 8c_h$ , we can rewrite  $w = \varepsilon - Ts + 2\mu q$  and thus the first law (4.15) can be written  $\delta\varepsilon = T\delta s - 2\mu\delta q$ .

The relevant terms for calculating the expectation value of the current are as in (3.20) and using (4.5), we obtain

$$\begin{aligned} \langle J_t \rangle &= 2q, \\ \langle J_{x_1} \rangle &= 2c_b, \end{aligned} \quad (4.17)$$

where we set  $f_0 = 1$ . From the temporal component we see that the constant  $q$  fixes the charge density and that, in general, there is current density in the  $x_1$  direction.

### 4.3.1 Variation of $w$ with respect to $k$

For a given temperature we are interested in the solution labelled by  $k_{min}$  which minimises the free energy. These black holes are specified by varying the action  $I_{Tot}$  with respect to  $k$ , putting it on-shell and then setting it to zero. We first note that

$$k \partial_k I_{Tot} = -Vol_3 \Delta\tau \int_{r_+}^{\infty} dr \frac{2k}{m} c_1 c_2. \quad (4.18)$$

One of the components of the gauge-field equation of motion, given in (A.8), implies that this integrand is a total derivative with respect to  $r$ , and hence can be easily evaluated. Substituting the asymptotic and near horizon expansions (4.5),(4.6) we find that at constant  $T$  we have

$$k\partial_k w = \frac{2k}{e}c_b. \quad (4.19)$$

We thus deduce that

$$\partial_k w = 0 \quad \Rightarrow \quad c_b = c_h = c_Q = 0. \quad (4.20)$$

where we used the Smarr formulae (4.13). In particular we see from (4.16) that the dual stress tensor for this one-parameter family of black hole solutions is homogeneous and isotropic with no momentum density in the  $x_1$  direction. In addition, from (4.17) we see that the current density in the  $x_1$  direction vanishes.

### 4.3.2 Connection with [31]

The general results of [31] for the thermodynamics of periodic black holes imply, in the present set-up, that

$$\begin{aligned} w &= -Ts - \bar{J}^t \mu + \bar{T}^{tt}, \\ w &= -\bar{T}^{x_2 x_2} = -\bar{T}^{x_3 x_3}, \\ w &= -T^{x_1 x_1} - J^{x_1} \bar{a}_{x_1}, \\ 0 &= -T^{x_1 t} + \mu \bar{J}^{x_1}, \\ \delta w &= -\bar{J}^t \delta \mu - s \delta T + \frac{\delta k}{k} (w + T^{x_1 x_1}), \end{aligned} \quad (4.21)$$

where  $a_{x_1}$  is a source term for the current and the bars refer to quantities averaged over a period in the  $x_1$  direction, as in section 3.3.2, and we have used the fact that stress energy conservation and current conservation imply  $T^{x_1 x_1}$ ,  $T^{t x_1}$  and  $J^{x_1}$  are constants. Using the actual expressions for the stress tensor and current given in (4.16), (4.17) and substituting into (4.21) we find that

$$\begin{aligned} w &= -Ts + 2q\mu + 3M + 8c_h, \\ w &= -M, \\ w &= -M - 8c_h + \frac{k}{e}2c_b, \\ 0 &= 4c_Q + 2c_b \mu, \\ \delta w &= 2q\delta\mu - s\delta T + \frac{\delta k}{k} (w + M + 8c_h), \end{aligned} \quad (4.22)$$

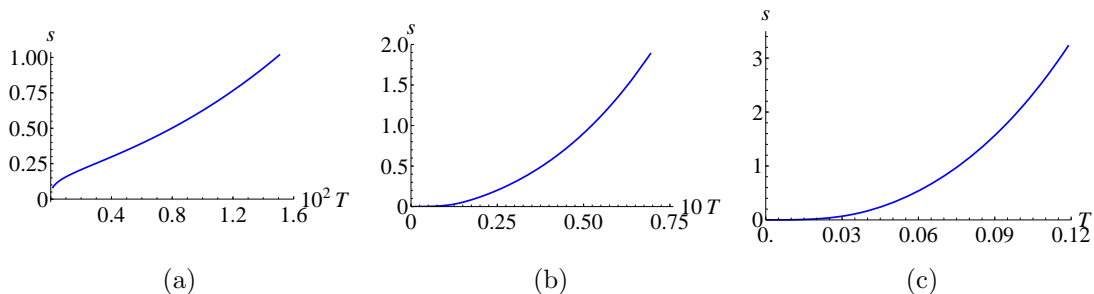


Figure 12: The low temperature behaviour of the entropy density  $s$  for the  $(p + ip)$ -wave black holes. The plots are for the thermodynamically preferred black holes in figure 2 with  $m = 2$  and  $e = 2$  (figure a),  $e = 2.8$  (figure b) and  $e = 3.5$  (figure c). Observe that for  $e = 2$  the zero entropy ground state behaviour only starts to appear for temperatures of the order  $10^{-3}$ . We have set  $\mu = 1$ .

thus recovering various expressions that we derived earlier. It is worth noting that in obtaining the third expression, which when combined with the second gives one of the Smarr-type formula in (4.13), we worked in the gauge where there was no phase in the two-form  $C$  but a source term appearing in the gauge-field: i.e.  $a_{x_1} = -k/e$ . If we wanted to work in the original gauge, with  $a_{x_1} = 0$ , we would need to extend the formalism of [31] to suitably take into account gauge-invariant variables.

### 4.3.3 Solutions with $k = 0$

We briefly comment on the  $k = 0$  branch of black holes. Recall that for suitably large  $e$ , such as  $e = 3.5$ , the thermodynamically preferred branch seems to cross the  $k = 0$  axis at very low temperatures. When  $k = 0$ , we deduce from (4.13) that  $c_h = 0$ . On the other hand, we find from our numerical results that  $c_Q$  and  $c_b$  are non-zero. In particular, from (4.19) we see that  $c_b = 0$  for the  $k = 0$  branch show that they are unstable. Unlike the  $p$ -wave case, there is no enhanced symmetry for the  $k = 0$  black holes and there is no additional consistent truncation.

## 4.4 Behaviour as $T \rightarrow 0$

For all of the  $(p + ip)$ -wave black holes we find that  $s \rightarrow 0$  as  $T \rightarrow 0$ , as we see in figure 12. It is worth noting that in some cases, for example  $m = 2$ ,  $e = 2$ , one has to go to temperatures of the order  $10^{-3}$  to see that the entropy density is in fact going to zero.

As yet, we have not been able to elucidate the nature of the ground state solutions as  $T \rightarrow 0$ . In particular, there do not seem to be analogues of the scaling solutions that we saw in the  $p$ -wave case, that we discussed in sections 3.6.1 and 3.6.2. However, it seems to be possible to construct domain wall solutions interpolating between  $AdS_5$  and itself using a similar expansion to what we considered in section 3.6.3, and these may play a key role. Indeed as  $r \rightarrow 0$ , we consider

$$\begin{aligned} g &= r^2 + \delta g, & f &= \bar{f}_0 + \delta f, & h &= h_0 r + \delta h, \\ Q &= Q_0 + \delta Q, & c_3 &= \delta c_3, & a &= a_0 + \delta a, & b &= b_0 + \delta b_0, \end{aligned} \quad (4.23)$$

where  $\bar{f}_0, h_0, Q_0, a_0$  and  $b_0$  are constants. After substituting into the equations of motion we find that at first order in the perturbation we just need to solve a second order linear ODE for  $\delta c_3$ . We find that the following solution can be developed:

$$\delta c_3 = c_3^0 \frac{e^{-kx/h_0 r}}{r^{1/2}} (1 + \mathcal{O}(r)), \quad (4.24)$$

where

$$x = \frac{(k - w_0 e)}{k} \sqrt{1 - \frac{h_0^2 (a_0 e + Q_0 (k - b_0 e))^2}{f_0^2 (k - b_0 e)^2}}. \quad (4.25)$$

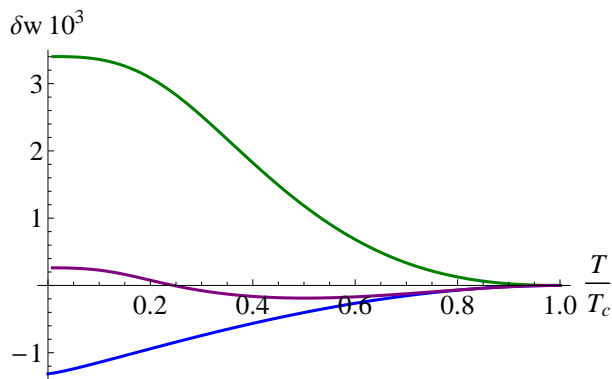
At next order in the perturbation we will get terms with  $e^{-2kx/h_0 r}$  appearing. This expansion is specified by six IR parameters. Combined with the seven UV parameters and two scaling symmetries from (4.4), we expect to find domain wall solutions that depend on one-parameter which can be taken to be  $k$ .

Finally, we point out that we can use the argument presented in section 3.7.5 to conclude that  $\partial_T k = 0$  as  $T \rightarrow 0$ . Indeed this is the behaviour we see in figures 10(b) and 10(c). This is not so immediate for figure 10(a) but further evidence can be obtained using a more detailed analysis of the low temperature limit.

## 5 $p$ -wave versus $(p + ip)$ -wave order

We have constructed  $p$ -wave and  $(p+ip)$ -wave black holes for  $m = 2$  and various values of  $e$ . In both cases the black holes have smaller free energy than that of the AdS-RN black holes and the transition from the AdS-RN phase to the thermodynamically preferred phase is second order, in each case.

We now compare the free energies for the  $p$ -wave and the  $(p + ip)$ -wave black holes. For  $e = 2$  we see in figure 13 that the  $p$ -wave black holes are preferred all



(a)

Figure 13: A plot of the difference,  $\delta w$ , of the free energy density of the  $p$ -wave and the  $(p + ip)$ -wave branches of thermodynamically preferred black holes (the red lines in figures 2 and 10). The plots are for  $m = 2$ . The blue curve is for  $e = 2$  and shows that the  $p$ -wave order is preferred for all  $T \leq T_c$ . The purple curve is for  $e = 2.8$  and shows that the  $p$ -wave order is first preferred and then there is a first order transition at  $T \sim 0.245T_c$  to the  $(p + ip)$ -wave order. The green curve is for  $e = 3.5$  and shows the  $(p + ip)$ -wave order is preferred for all  $T \leq T_c$ . We have set  $\mu = 1$ .

the way down to zero temperature. As the value of  $e$  is increased, the  $(p + ip)$ -wave become more favourable. Our numerical results indicate that at some critical value of  $e$ , whose precise value is hard to establish, the branches meet at  $T = 0$  (i.e. they have the same free energy - the solutions seem to be distinct). Increasing  $e$  a little further we get to the situation exemplified by  $e = 2.8$  in figure 13. In this case there is a second order phase transition from the AdS-RN black holes to the  $p$ -wave black holes, followed by a first order transition to the  $(p + ip)$ -wave black holes. Beyond another critical value of  $e$  the  $p$ -wave branch is never preferred and there is just a second order transition from the AdS-RN black holes to the  $(p + ip)$ -wave black holes. This is illustrated for  $e = 3.5$  in figure 13.

The phase structure that we have found for  $m = 2$  and various  $e$  implies that the phenomenon of pitch inversion that we saw for the  $p$ -wave branches is not thermodynamically preferred. Furthermore, for  $m = 2$  we find that of the three types of  $T = 0$  ground states for the  $p$ -wave black holes which we discussed in sections 3.6 and 3.7, only the Bianchi VII<sub>0</sub> scaling solutions are preferred. It is quite possible that the situation changes for different values of  $m$ . Another open issue is whether the  $p$ -wave and  $(p + ip)$ -wave black holes themselves are unstable. If they are, then they will

sprout additional black hole branches (as in [23]) which could modify the conclusions concerning the phase structure.

## 6 Discussion

Building on [20, 21] we have investigated in further detail the  $p$ -wave and  $(p + ip)$ -wave superconducting black holes that arise in a  $D = 5$  theory of gravity coupled to a gauge-field and a charged two-form. The model depends on two-parameters,  $m$  and  $e$  and we focussed on the case  $m = 2$  and then varied  $e$ . For the  $p$ -wave black holes, for some values of  $e$  we again saw some of the features seen in [21] for  $m = 1.7$  and  $e = 1.88$ . For example, when  $e = 2$  the zero temperature black holes approach ground states which are domain walls interpolating between  $AdS_5$  in the UV and a Bianchi VII<sub>0</sub> scaling solution in the IR. For other values of  $e$  we saw some new features. Firstly, when  $e \gtrsim 2.9$  the thermodynamically preferred black holes exhibit the phenomenon of pitch inversion. Secondly, when  $e \sim 2.9$  the zero temperature limits of the black holes appear to approach domain walls interpolating from  $AdS_5$  in the UV and a novel anisotropic scaling solution in the IR with  $k = 0$ . For larger values of  $e$  the ground state solutions appear to interpolate between  $AdS_5$  in the UV and  $AdS_5$  in the IR. It will be particularly interesting to explore this latter class of domain walls in more detail. For example, based on [37], one might expect that they will have conductivities with novel properties.

The back-reacted  $(p + ip)$ -wave black holes, depending on wave number  $k$  that we constructed here are new. The  $(p + ip)$ -wave black holes also approach zero temperature ground states with vanishing entropy. While we have not been able to identify the ground states that occur in this case, we argued that there are possible domain wall solutions interpolating between the same  $AdS_5$  in the UV and the IR, which may play an important role. We analysed the competition between the different orders and found that for low values of  $e$  the  $p$ -wave order is preferred, but for higher values  $(p + ip)$ -wave order is preferred. For intermediate values of  $e$  there is a first order transition from the  $p$ -wave to the  $(p + ip)$ -wave order.

Finally, it would be interesting to carry out similar investigations into the  $p$ -wave and  $(p + ip)$ -wave black holes that arise in theories of gravity coupled to  $SU(2)$  gauge-fields extending [4–6, 8]. In particular, we expect that analogously rich classes of black solutions and ground states will be present for the  $D = 5$  models studied in [20] (that developed the work of [41]). It would also be of interest to investigate the interplay of helical magnetic orders and superconductivity, that have been discussed in [42, 43],

within a holographic context.

## Acknowledgements

We thank A. Green, S. Hartnoll and J. Sonner for helpful discussions. The work is supported by STFC grant ST/J0003533/1 and also by the European Research Council under the European Union’s Seventh Framework Programme (FP7/2007-2013), ERC Grant agreement STG 279943, “Strongly Coupled Systems”. CP is supported by an I.K.Y. Scholarship.

## A Smarr formulae for the $(p + ip)$ -wave black holes

For an arbitrary Killing vector  $\zeta^a$  we have

$$R^a{}_b \zeta^b = \nabla_b \nabla^a \zeta^b. \quad (\text{A.1})$$

Since the metric ansatz (4.1) depends only on the radial coordinate  $r$ , this can be rewritten

$$R^a{}_b \zeta^b = -\frac{1}{\sqrt{-g}} \partial_r [\sqrt{-g} \nabla^r \zeta^a], \quad (\text{A.2})$$

and we obtain

$$\begin{aligned} \sqrt{-g} R^t{}_t &= -\partial_r (r^2 g h f' + \frac{1}{2} r^2 f h g' - \frac{r^2 h^3 Q Q'}{2f}), \\ \sqrt{-g} R^{x_1}{}_t &= \partial_r (r^2 g h Q f' + \frac{1}{2} r^2 f h Q g' - r^2 f g Q h' - \frac{1}{2} r^2 f g h Q' - \frac{r^2 h^3 Q^2 Q'}{2f}), \\ \sqrt{-g} R^{x_1}{}_{x_1} &= -\partial_r (r^2 f g h' + \frac{r^2 h^3 Q Q'}{2f}), \\ \sqrt{-g} R^{x_2}{}_{x_2} &= -\partial_r (r f g h), \end{aligned} \quad (\text{A.3})$$

where the first two equations arise from the Killing vector  $\partial_t$  and the next two equations arise from the Killing vectors  $\partial_{x_1}$  and  $\partial_{x_2}$ , respectively. As in [44] the strategy to obtain the Smarr formula is to use the equations of motion (2.3) to find linear combinations of these four equations so that the left hand side is also a total derivative.

We first write the Einstein equations appearing in (2.3) as

$$R_{\mu\nu} = -4g_{\mu\nu} + X_{\mu\nu}^{(F)} + X_{\mu\nu}^{(C)}, \quad (\text{A.4})$$

where

$$\begin{aligned} X_{\mu\nu}^{(F)} &= \frac{1}{2} \left( F_{\mu}{}^{\rho} F_{\nu\rho} - \frac{1}{6} g_{\mu\nu} F_{\rho\sigma} F^{\rho\sigma} \right) , \\ X_{\mu\nu}^{(C)} &= \frac{1}{2} \left( C_{(\mu}{}^{\rho} \bar{C}_{\nu)\rho} - \frac{1}{6} g_{\mu\nu} C_{\rho\sigma} \bar{C}^{\rho\sigma} \right) . \end{aligned} \quad (\text{A.5})$$

Let us focus on the components  $X^{(F)i}{}_j$  where  $i, j$  run over the coordinates  $t, x_1, x_2, x_3$ . Since the gauge-field in our ansatz has the form  $A = a_i(r) dx^i$  we have

$$\begin{aligned} \sqrt{-g} X^{(F)i}{}_j &= \frac{1}{2} \sqrt{-g} \left( F^{ri} \delta_j^k - \frac{1}{3} F^{rk} \delta_j^i \right) \partial_r a_k , \\ &= \partial_r \left[ \frac{1}{2} \sqrt{-g} \left( F^{ri} \delta_j^k - \frac{1}{3} F^{rk} \delta_j^i \right) a_k \right] \\ &\quad - \frac{1}{2} \left[ \partial_r \left( \sqrt{-g} F^{ri} \right) \delta_j^k - \frac{1}{3} \partial_r \left( \sqrt{-g} F^{rk} \right) \delta_j^i \right] a_k . \end{aligned} \quad (\text{A.6})$$

We can then rewrite the last line using the following equations of motion for the gauge-field

$$\partial_r \left( \sqrt{-g} F^{ri} \right) = -\frac{e}{4m} \sqrt{-g} \epsilon^{irjkl} \left[ C_{rj} \bar{C}_{kl} + \bar{C}_{rj} C_{kl} \right] . \quad (\text{A.7})$$

The right hand side of this expression contains terms that are quadratic in the functions  $c_1, c_2$  and  $c_3$ , as does  $\sqrt{-g} X^{(C)i}{}_j$ . In fact the only non-trivial relations in (A.7) are given by

$$\begin{aligned} \partial_r \left( \sqrt{-g} F^{rt} \right) &= -\frac{2e}{m} c_2 c_3 , \\ \partial_r \left( \sqrt{-g} F^{rx_1} \right) &= \frac{2e}{m} c_1 c_2 . \end{aligned} \quad (\text{A.8})$$

The last step is to use the equation of motion for the two-form  $C$  to find linear combinations where the terms that are quadratic in the  $c_i$  can be expressed as a total derivative with respect to  $r$ . The  $(r, t, x_2)$  and  $(r, x_1, x_2)$  components of the equation of motion  $H = -im * C$  can be written as

$$\begin{aligned} \partial_r c_1 &= eac_2 - \frac{m}{fgh} \left( h^2 Q c_1 + (f^2 g - h^2 Q^2) c_3 \right) , \\ \partial_r c_3 &= (eb - k) c_2 - \frac{mh}{fg} (c_1 - Q c_3) . \end{aligned} \quad (\text{A.9})$$

It is also useful to note that the equation of motion for  $C$  also implies that  $c_2$  can be solved algebraically in terms of  $c_1$  and  $c_3$ :

$$c_2 = \frac{1}{m f g h} \left( eac_3 - (eb - k) c_1 \right) , \quad (\text{A.10})$$

as one can deduce from (4.3).

After combining these ingredients, it is straightforward to show that the relevant linear combinations are given by

$$\begin{aligned}
\sqrt{-g}(R^t_t - R^{x_2}_{x_2}) &= \partial_r \left( \frac{1}{2} \sqrt{-g} a F^{rt} + \frac{1}{2m} c_1 c_3 \right), \\
\sqrt{-g}(R^{x_1}_{x_1} - R^{x_2}_{x_2}) &= \partial_r \left( \frac{1}{2} \sqrt{-g} \left( b - \frac{k}{e} \right) F^{rx_1} - \frac{1}{2m} c_1 c_3 \right), \\
\sqrt{-g} R^{x_1}_t &= \partial_r \left( \frac{1}{2} \sqrt{-g} a F^{rx_1} - \frac{1}{2m} c_1 c_1 \right).
\end{aligned} \tag{A.11}$$

Combining equations (A.3) with (A.11) we can then integrate from  $r = r_+$  to  $r = \infty$ . After substituting in the asymptotic (4.5) and near horizon (4.6) expansions, we obtain three Smarr-type formulae given by

$$\begin{aligned}
4M + 8c_h + 2\mu q - sT &= 0, \\
4c_h - \frac{k}{e} c_b &= 0, \\
2c_Q + c_b \mu &= 0.
\end{aligned} \tag{A.12}$$

where we have set  $f_0 = 1$ . These are the formulae (4.12) and (4.13) stated in the main text for the  $(p + ip)$ -wave black holes.

## References

- [1] S. S. Gubser, “Breaking an Abelian Gauge Symmetry Near a Black Hole Horizon,” *Phys. Rev.* **D78** (2008) 065034, [arXiv:0801.2977 \[hep-th\]](#).
- [2] S. A. Hartnoll, C. P. Herzog, and G. T. Horowitz, “Building a Holographic Superconductor,” *Phys. Rev. Lett.* **101** (2008) 031601, [arXiv:0803.3295 \[hep-th\]](#).
- [3] S. A. Hartnoll, C. P. Herzog, and G. T. Horowitz, “Holographic Superconductors,” *JHEP* **12** (2008) 015, [arXiv:0810.1563 \[hep-th\]](#).
- [4] S. S. Gubser, “Colorful horizons with charge in anti-de Sitter space,” *Phys.Rev.Lett.* **101** (2008) 191601, [arXiv:0803.3483 \[hep-th\]](#).
- [5] S. S. Gubser and S. S. Pufu, “The Gravity dual of a p-wave superconductor,” *JHEP* **0811** (2008) 033, [arXiv:0805.2960 \[hep-th\]](#).

- [6] M. M. Roberts and S. A. Hartnoll, “Pseudogap and time reversal breaking in a holographic superconductor,” *JHEP* **0808** (2008) 035, [arXiv:0805.3898](#) [hep-th].
- [7] F. Aprile, D. Rodriguez-Gomez, and J. G. Russo, “p-wave Holographic Superconductors and five-dimensional gauged Supergravity,” *JHEP* **01** (2011) 056, [arXiv:1011.2172](#) [hep-th].
- [8] M. Ammon, J. Erdmenger, V. Grass, P. Kerner, and A. O’Bannon, “On Holographic p-wave Superfluids with Back-reaction,” *Phys.Lett.* **B686** (2010) 192–198, [arXiv:0912.3515](#) [hep-th].
- [9] J.-W. Chen, Y.-J. Kao, D. Maity, W.-Y. Wen, and C.-P. Yeh, “Towards A Holographic Model of D-Wave Superconductors,” *Phys.Rev.* **D81** (2010) 106008, [arXiv:1003.2991](#) [hep-th].
- [10] F. Benini, C. P. Herzog, R. Rahman, and A. Yarom, “Gauge gravity duality for d-wave superconductors: prospects and challenges,” *JHEP* **1011** (2010) 137, [arXiv:1007.1981](#) [hep-th].
- [11] K.-Y. Kim and M. Taylor, “Holographic d-wave superconductors,” *JHEP* **1308** (2013) 112, [arXiv:1304.6729](#) [hep-th].
- [12] S. Nakamura, H. Ooguri, and C.-S. Park, “Gravity Dual of Spatially Modulated Phase,” *Phys. Rev.* **D81** (2010) 044018, [arXiv:0911.0679](#) [hep-th].
- [13] A. Donos and J. P. Gauntlett, “Black holes dual to helical current phases,” *Phys.Rev.* **D86** (2012) 064010, [arXiv:1204.1734](#) [hep-th].
- [14] A. Donos and J. P. Gauntlett, “Holographic striped phases,” *JHEP* **1108** (2011) 140, [arXiv:1106.2004](#) [hep-th].
- [15] M. Rozali, D. Smyth, E. Sorkin, and J. B. Stang, “Holographic Stripes,” *Phys.Rev.Lett.* **110** (2013) 201603, [arXiv:1211.5600](#) [hep-th].
- [16] A. Donos, “Striped phases from holography,” *JHEP* **1305** (2013) 059, [arXiv:1303.7211](#) [hep-th].
- [17] B. Withers, “Black branes dual to striped phases,” [arXiv:1304.0129](#) [hep-th].

- [18] B. Withers, “The moduli space of striped black branes,” [arXiv:1304.2011](#) [[hep-th](#)].
- [19] A. Donos and J. P. Gauntlett, “Holographic charge density waves,” [arXiv:1303.4398](#) [[hep-th](#)].
- [20] A. Donos and J. P. Gauntlett, “Holographic helical superconductors,” *JHEP* **12** (2011) 091, [arXiv:1109.3866](#) [[hep-th](#)].
- [21] A. Donos and J. P. Gauntlett, “Helical superconducting black holes,” *Phys.Rev.Lett.* **108** (2012) 211601, [arXiv:1203.0533](#) [[hep-th](#)].
- [22] P. Basu, J. He, A. Mukherjee, M. Rozali, and H.-H. Shieh, “Competing Holographic Orders,” *JHEP* **1010** (2010) 092, [arXiv:1007.3480](#) [[hep-th](#)].
- [23] A. Donos and J. P. Gauntlett, “Superfluid black branes in  $AdS_4 \times S^7$ ,” *JHEP* **06** (2011) 053, [arXiv:1104.4478](#) [[hep-th](#)].
- [24] A. Donos, J. P. Gauntlett, J. Sonner, and B. Withers, “Competing orders in M-theory: superfluids, stripes and metamagnetism,” *JHEP* **1303** (2013) 108, [arXiv:1212.0871](#) [[hep-th](#)].
- [25] D. Musso, “Competition/Enhancement of Two Probe Order Parameters in the Unbalanced Holographic Superconductor,” *JHEP* **1306** (2013) 083, [arXiv:1302.7205](#) [[hep-th](#)].
- [26] R.-G. Cai, L. Li, L.-F. Li, and Y.-Q. Wang, “Competition and Coexistence of Order Parameters in Holographic Multi-Band Superconductors,” *JHEP* **1309** (2013) 074, [arXiv:1307.2768](#) [[hep-th](#)].
- [27] F. Nitti, G. Policastro, and T. Vanel, “Dressing the Electron Star in a Holographic Superconductor,” [arXiv:1307.4558](#) [[hep-th](#)].
- [28] Y. Liu, K. Schalm, Y.-W. Sun, and J. Zaanen, “Bose-Fermi competition in holographic metals,” [arXiv:1307.4572](#) [[hep-th](#)].
- [29] Z.-Y. Nie, R.-G. Cai, X. Gao, and H. Zeng, “Competition between the s-wave and p-wave superconductivity phases in a holographic model,” [arXiv:1309.2204](#) [[hep-th](#)].
- [30] I. Amado, D. Arean, A. Jimenez-Alba, L. Melgar, and I. S. Landea, “Holographic s+p Superconductors,” [arXiv:1309.5086](#) [[hep-th](#)].

- [31] A. Donos and J. P. Gauntlett, “On the thermodynamics of periodic AdS black branes,” [arXiv:1306.4937](#) [hep-th].
- [32] N. Iizuka, S. Kachru, N. Kundu, P. Narayan, N. Sircar, *et al.*, “Bianchi Attractors: A Classification of Extremal Black Brane Geometries,” *JHEP* **1207** (2012) 193, [arXiv:1201.4861](#) [hep-th].
- [33] M. Taylor, “Non-relativistic holography,” [arXiv:0812.0530](#) [hep-th].
- [34] P. Chesler, A. Lucas, and S. Sachdev, “Conformal field theories in a periodic potential: results from holography and field theory,” [arXiv:1308.0329](#) [hep-th].
- [35] V. Balasubramanian and P. Kraus, “A stress tensor for anti-de Sitter gravity,” *Commun. Math. Phys.* **208** (1999) 413–428, [arXiv:hep-th/9902121](#).
- [36] S. S. Gubser and A. Nellore, “Ground states of holographic superconductors,” *Phys.Rev.* **D80** (2009) 105007, [arXiv:0908.1972](#) [hep-th].
- [37] G. T. Horowitz and M. M. Roberts, “Zero Temperature Limit of Holographic Superconductors,” *JHEP* **0911** (2009) 015, [arXiv:0908.3677](#) [hep-th].
- [38] P. Basu, J. He, A. Mukherjee, and H.-H. Shieh, “Hard-gapped Holographic Superconductors,” *Phys.Lett.* **B689** (2010) 45–50, [arXiv:0911.4999](#) [hep-th].
- [39] S. A. Hartnoll, J. Polchinski, E. Silverstein, and D. Tong, “Towards strange metallic holography,” *JHEP* **1004** (2010) 120, [arXiv:0912.1061](#) [hep-th].
- [40] M. Rozali, D. Smyth, E. Sorkin, and J. B. Stang, “Striped Order in AdS/CFT,” *Phys.Rev.* **D87** (2013) 126007, [arXiv:1304.3130](#) [hep-th].
- [41] L. A. Pando Zayas and D. Reichmann, “A Holographic Chiral  $p_x + ip_y$  Superconductor,” *Phys.Rev.* **D85** (2012) 106012, [arXiv:1108.4022](#) [hep-th].
- [42] T. Neupert and M. Sgrist, “Coexistence of ferromagnetism and superconductivity in noncentrosymmetric materials with cubic symmetry,” *J.Phys.Soc.Jpn.* **80** (2011) 114712.
- [43] G. J. Conduit, C. J. Pedder, and A. G. Green, “Fluctuation-induced pair density wave in itinerant ferromagnets,” *Phys.Rev* **B87** (2013) 121112, [arXiv:1303.4745](#) [cond-mat.str-el].

- [44] J. Bhattacharya, S. Bhattacharyya, and S. Minwalla, “Dissipative Superfluid dynamics from gravity,” *JHEP* **1104** (2011) 125, [arXiv:1101.3332 \[hep-th\]](#).